**CHULALONGKORN UNIVERSITY**

**RATCHADAPHISEKSOMPHOT ENDOWMENT FUND**

**FINAL REPORT**

# Cytotoxic constituents from *Dendrobium* spp.


**Investigators**

**Associate Professor Dr. Boonchoo Sritularak**

**Professor Dr. Kittisak Likhitwitayawuid**

**Associate Professor Dr. Pithi Chanvorachote**

**Assistant Dr. Varisa Pongrakhananon**


**August 2014**

## ABSTRACT

The MeOH extracts of *Dendrobium pullchellum* Roxb. ex Lindl. and *D. ellipsophyllum* Tang & wang (Orchidaceae) showed significant cytotoxic activity against human lung cancer cells. Phytochemical study of the whole plant of *D. pullchellum* Roxb. ex Lindl led to the isolation of seven phenolic compounds, namely, chrysotobibenzyl, chrysotoxine, crepidatin, moscatilin, fimbriatone, (-)-shikimic acid and liriodendrin. The whole plant of *D. ellipsophyllum* Tang & wang yielded ten phenolic compounds including moscatilin, 5,7-dihydroxy-chromen-4-one, 4,5-dihydroxy-2,3-dimethoxy-9,10-dihydrophenanthrene, 4,4′-dihydroxy-3,5-dimethoxybibenzyl, 4,5,4′-trihydroxy-3,3′-dimethoxybibenzyl, (2*S*)-homoeriodictyol, (2*S*)-eriodictyol, chrysoeriol, phloretic acid and luteolin. The structures of all these isolates were determined by extensive spectroscopic studies, including comparison of their MS and NMR properties with previously reported data. Each of these isolates was evaluated for cytotoxic and anti-metastatic activities against human lung cancer cells. It was found that chrysotobibenzyl, chrysotoxine, crepidatin, moscatilin, 4,4′-dihydroxy-3,5-dimethoxybibenzyl, 4,5,4′-trihydroxy-3,3′-dimethoxybibenzyl, chrysoeriol and luteolin exhibited appreciable cytotoxic and anti-metastatic effects. Moscatilin, the strongest cytotoxic compound, was further evaluated for its mechanisms of action on human lung cancer cell migration and invasion. The present study demonstrates that the inhibitory effect of moscatilin was associated with an attenuation of endogenous reactive oxygen species (ROS), in which hydroxyl radical ($OH^{\bullet}$) was identified as a dominant species in the suppression of filopodia formation.

# ABSTRACT (THAI)

สิ่งสกัดหยาบชั้นเมทานอลของเอื้องช้างน้าวและเอื้องทอง (วงศ์กล้วยไม้) มีฤทธิ์ยับยั้งเซลล์มะเร็งปอดของมนุษย์อย่างมีนัยสำคัญ การศึกษาทางพฤกษเคมีของส่วนทั้งต้นของเอื้องช้างน้าว พบสารกลุ่มฟีนอลิก 7 ชนิด ได้แก่ chrysotobibenzyl, chrysotoxine, crepidatin, moscatilin, fimbriatone, (-)-shikimic acid และ liriodendrin การศึกษาทางพฤกษเคมีของส่วนทั้งต้นของเอื้องทอง แยกสารกลุ่มฟีนอลิกได้ 10 ชนิด คือ moscatilin, 5,7-dihydroxy-chromen-4-one, 4,5-dihydroxy-2,3-dimethoxy-9,10-dihydrophenanthrene, 4,4′-dihydroxy-3,5-dimethoxybibenzyl, 4,5,4′-trihydroxy-3,3′-dimethoxybibenzyl, (2*S*)-homoeriodictyol, (2*S*)-eriodictyol, chrysoeriol, phloretic acid และ luteolin การพิสูจน์โครงสร้างทางเคมีของสารที่แยกได้นี้ อาศัยการวิเคราะห์สเปคตรัมของ MS และ NMR ร่วมกับการเปรียบเทียบข้อมูลของสารที่ทราบโครงสร้างแล้ว ได้ทำการทดสอบฤทธิ์เป็นพิษและฤทธิ์ยับยั้งการแพร่กระจายของเซลล์มะเร็งปอดของมนุษย์ของสารแต่ละชนิด พบว่าสารที่มีฤทธิ์ได้แก่ chrysotobibenzyl, chrysotoxine, crepidatin, moscatilin, 4,4′-dihydroxy-3,5-dimethoxybibenzyl, 4,5,4′-trihydroxy-3,3′-dimethoxybibenzyl, chrysoeriol และ luteolin เมื่อนำ moscatilin ซึ่งเป็นสารที่มีความเป็นพิษต่อเซลล์มะเร็งปอดที่แรงที่สุด มาศึกษากลไกการยับยั้งการเคลื่อนที่และการรุกล้ำของเซลล์มะเร็งปอด พบว่าผลการยับยั้งของ moscatilin มีความสัมพันธ์กับการลดระดับของอนุพันธ์ออกซิเจนที่ว่องไวภายในเซลล์โดยพบว่าไฮดรอกซิลเป็นอนุพันธ์ที่สำคัญในการลดการเกิดฟีโลโพเดีย

# CONTENTS

## CONTENT (continued)

# LIST OF FIGURES

# LIST OF TABLES

# INTRODUCTION

Cancer is a disease caused by cell proliferation with uncontrollable rate. According to the data collected between 2005-2009 on the number of deaths and death rates per 100,000 populations, malignant neoplasm or cancer in all forms is the first-ranked cause of death in Thailand (Bureau of Policy and Strategy, Ministry of Public Health, 2009). There are several approaches in the treatment of cancer including radiation, chemotherapy and surgery or combinations to increase the efficiency of the therapy. Some drugs that are used to treat cancer are originated from natural sources, such as vincristine, vinblastine and paclitaxel. However, discovery of new drugs with higher efficacy and safety for cancer treatment is still needed since most patients treated with chemotherapy cannot tolerate side effects of currently used drugs.

Despite advances in cancer chemotherapy, research into new treatment strategies is still needed. It has been widely accepted that most cancer-related deaths are caused by metastasis, and the search for compounds that possess the ability to inhibit such cancer behavior is considered necessary. Among various steps of cancer metastasis, resistance to anoikis, a cellular process of apoptosis induced by cell detachment, is known to be a critical ability of cancer cells to ensure successful metastasis (Chiarugi and Giannoni, 2008; Boisvert *et al*., 2009). Indeed, once cells are detached from the extracellular matrix, the loss of cell adhesion triggers dramatic reduction of cellular signals controlling survival and growth (Hynes, 1999) and mediates the anoikis process (Frisch and Francis, 1994). Likewise, the ability of cancer cells to grow in a detached condition has been shown to be tightly related with the degree of cancer metastasis, as well as cancer aggressiveness (Hanahan and Weinberg, 2000; Shanmugathasan and Jothy, 2000; Mori *et al*., 2009). So far, only a few anti-metastatic agents from natural sources have been

reported, such as emodin from rhubarb (Huang *et al*., 2007) and curcusone B, a diterpene, from *Jatropha curcas* (Muangman *et al*., 2005).

*Dendrobium* is the biggest genus of orchids, represented by more than 1,100 species. The plants of this genus are either epiphytic, or occasionally lithophytic. These plants have adapted to a wide variety of habitats and distributed throughout Asia and Australia (Seidenfaden, 1985; Guanghua *et al*., 2009). The stems of several *Dendrobium* species have been used in traditional Chinese medicines as tonics to reduced fever and promote the production of body fluid (Hu *et al*., 2012).

Previous pharmacological studies have been shown that some *Dendrobium* species were potential sources of cytotoxic compounds (Ng *et al*., 2012). Several cytotoxic constituents from this plant have been reported, for example, dengraols A and B from *D. gratiosissimum* (Zhang *et al*., 2008), erianin, a potent cytotoxic compound against human leukemia HL-60 cells, from *D. chrysotoxum* (Li *et al*., 2001), and moscatilin, a known cytotoxic compound previously reported from several other *Dendrobium* species (Ho and Chen, 2003).

According to our previous studies, chemical constituents in plants of the genus *Dendrobium* could be classified into several groups, including, bibenzyls, bisbibenzyls, phenanthrene, dihydrophenanthrenes, lignans, phenylpropanoids and flavonoids (Sritularak and Likhitwitayawuid 2009; Sritularak *et al*. 2011a; Sritularak *et al*, 2011b; Phechrmeekha *et al*., 2012). In this study, screening for cytotoxic activity against lung cancers of some *Dendrobium* plant extracts was carried out and the MeOH extracts of *D. pullchellum* Roxb. ex Lindl. and *D. ellipsophyllum* Tang & wang showed appreciable activity. These plants were a native plant of Thailand with no previous reports on their secondary metabolites. These preliminary observations prompted us to conduct an investigation on the extract of these plants in order to find the compounds responsible

for cytotoxic activity. Moreover, moscatilin, the strongest cytotoxic compound from *D. pulchellum*, was further evaluated for its mechanisms of action on human lung cancer cell migration and invasion. Moscatilin is only one compound which was found from all species of the plant samples.

The overall objectives of this research program are put forward, as follows:

(1) To screen cytotoxic activity of some *Dendrobium* plant extracts such as *D. ellipsophyllum*, *D. venustum*, *D. lindleyi*, *D. brymerianum*, *D. williamsonii*, *D. densiflorum*, *D. pulchellum*, *D. signatum*.

(2) To isolate pure compounds from a selected *Dendrobium* spp. and identify of the chemical structure of each isolated compound.

(3) To evaluate of each isolated compound for its cytotoxic and anti-metastatic activities.

(4) To evaluate mechanisms of action of moscatilin on human lung cancer cell migration and invasion.

Therefore, this research program is comprised of 2 main projects, as follow:

(1) Search for cytotoxic and anti-metastatic agents from *Dendrobium* spp. (Figure 1)

1.1 Cytotoxic and anti-metastatic activities of compounds from *D. pulchellum*

1.2 Cytotoxic and anti-metastatic activities of compounds from *D. ellipsophyllum*

(2) Evaluation for mechanism of action of moscatilin against human lung cancer cells.

**A**

**B**

**Figure 1** (A) *D. pulchellum* (B) *D. ellipsophyllum*

## SURVEY OF RELATED LITERATURE

*Dendrobium* is the biggest genus of orchids, represented by more than 1,100 species. The plants of this genus are either epiphytic, or occasionally lithophytic. These plants have adapted to a wide variety of habitats and distributed throughout Asia and Australia (Seidenfaden, 1985; Guanghua *et al*., 2009).

Several plants in the genus *Dendrobium* have beautiful flowers and are widely cultivated as decorative plants. In China they are also used in traditional medicine to treat kidney, lung and stomach diseases, fever, red tongue, dry mouth, swelling, hyperglycaemia, atrophic gastritis and diabetes (Hossain, 2011). A well-known formulation, "Shi-Hu" (Herba Dendrobii), consists of dry or fresh stems of several *Dendrobium* species including *D. loddigesii*, *D. fimbriatum*, *D. chrysanthum*, *D. candidum* and *D. nobile*.

Several biological activities have been reported for plants in the genus *Dendrobium*, for example, cytotoxic, antioxidative, antiinflammatory, antiplatelet aggregation and spasmolytic properties.

Up to now, several cytotoxic constituents from *Dendrobium* plant have been reported. Examples of cytotoxic compounds from *Dendrobium* plants are coelonin and denbinobin from *D. nobile* could inhibit the proliferation of hepatic stellate cell (HSCs-T6), involved in liver fibrosis (Yang *et al*., 2007). Denthyrsin from *D. thyrsiflorum* exhibited cytotoxicity against several cancer cell lines including Hela, K-562, MCF-7 (Zhang *et al*., 2005). The bibenzyl moscatilin, isolated from several plants of this genus, showed strong cytotoxicity against several cancer cell lines. In addition, this compound was able to induce apoptosis in colorectal cancer cell lines through tubulin depolymerization and DNA damage stress, these results led to the activation of C-Jun $NH_2$-terminal protein kinase (JNK) and mitochondria-involved intrinsic apoptosis

pathway (Chen *et al*., 2008a). Moscatilin also showed anti-angiogenic effect *in vitro* and *in vivo* by inhibiting angiogenic factor signaling pathways (Tsai *et al.*, 2010). From the literature review, therefore, *Dendrobium* species were potential sources of cytotoxic compounds.

## PROCEDURES

### General procedures

NMR spectra were obtained with a Bruker Avance DPX-300 FT-NMR spectrometer (Bruker, Rheinstetten, Germany). Mass spectra were recorded on either a Bruker microTOF (Bruker Daltonics, Bremen, Germany) or a Micromass LCT mass spectrometer (Micromass, Manchester, UK). Vacuum liquid column chromatography (VLC) and CC were performed with silica gel 60 (70-230 mesh, Merck, Darmstadt, Germany), and silica gel 60 (230-400 mesh, Merck), respectively. MCI Gel CHP20P and Sephadex LH-20 (particle size 25-100 μm) were manufactured by Supelco (Bellefonte, PA) and Pharmacia Fine Chemicals (Uppsala, Sweden), respectively.

### Plant materials

The samples of *D. pulchellum* and *D. ellipsophyllum* were purchased from Jatujak market, Bangkok, Thailand in June 2009 and May 2012, respectively. These plants were identified by Prof. Thatree Phadungcharoen (Department of Pharmacognosy and Pharmaceutical Botany, Faculty of Pharmaceutical Sciences, Chulalongkorn University, Bangkok, Thailand) and were confirmed by comparison with herbarium specimens at the Department of National Park, Wildlife and Plant Conservation, Ministry of National Resources and Environment.

**Cells and reagents**

Human lung cancer H23 and H292 cells were obtained from the American Type Culture Collection (Manassas, VA). Cells were cultured in RPMI 1640 containing 5% fetal bovine serum, 2 mM L-glutamine, and 100 units/mL penicillin/streptomycin in a 5% $CO_2$ environment at 37°C. 2,3-Bis(2-methoxy-4-nitro-5-sulfophenyl)-2H-tetrazolium-5-carboxanilide (XTT), and other chemicals were obtained from Sigma Chemical, Inc. (St. Louis, MO). Hoechst 33342 were obtained from Molecular Probes, Inc (Eugene, OR). The Hoechst 33342, propidium iodide (PI), phalloidin tetramethylrhodamine B isothiocyanate, ribonuclease A, bovine serum albumin (BSA) and dimethysulfoxide (DMSO) were purchased from Sigma Chemical, Inc. (St. Louis, MO, USA). Annexin V Apoptosis Detection Kit was obtained from BD Biosciences (Woburn,MA,USA). Antibodies for phosphorylated Akt (S473), Akt, phosphorylated FAK (Y397), FAK, phosphorylated ERK (Thr202/Tyr204), ERK, Cdc42, β-actin and peroxidase-conjugated secondary antibodies were obtained from Cell Signaling (Denvers, MA, USA)

**Cell viability assays**

Cell viability was determined by MTT or XTT assays as previously described (Chanvorachote and Pongrakhananon, 2013). Initially, cells were seeded at a density of $10^4$ cells/well onto 96-well plate overnight. After that, they were treated with various concentrations of moscatilin for 24 h. The medium was then replaced with MTT solution (5.0 mg/mL in PBS) and incubated at 37°C for 4 h. To solubilize formazan product, the medium was replaced with 100 µl DMSO, and an intensity reading of the formazan product was measured at 550 nm using a microplate reader (Anthros, Durham, NC, USA). Cell viability was expressed as the percentage calculated from absorbance of MTT-treated cells relative to control cells. For XTT assay, cells were harvested, washed,

and incubated with 20 μM of 2,3-Bis(2-methoxy-4-nitro-5-sulfophenyl)-2H-tetrazolium-5-carboxanilide (XTT) for 4 h at 37°C. Optical density was then determined with a V-max photometer (Molecular Devices Inc., Menlopark, CA) at a wavelength of 450 nm.

**Anoikis assay**

To prevent cell adhesion, tissue culture 6-well plates were coated with 200 μL (6 mg/mL in 95% ethanol) of poly (2-hydroxyethyl methacrylate) (poly-HEMA; Sigma) and left to dry overnight in a laminar flow hood at room temperature. Adherent H23 cells in culture plate were trypsinized into a single cell suspension in RPMI medium and then seeded in Poly-HEMA-coated plates at a density of $1\times10^5$ cells/mL. Suspended cells were incubated at 37°C for various times up to 24 h.

**Colony formation assay**

Anchorage-independent growth was determined by a colony formation assay in soft agar. Lung cancer cells were prepared into a single-cell suspension by treatment with a mixture of 350 μL trypsin and 1.5 mM EDTA. Cells were suspended in RPMI containing 10% FBS and 0.33% low melting temperature agarose. Then a 2 mL suspension containing $2\times10^4$ cells was placed in a 35 mm dish over a 3 mL layer of solidified RPMI/10% FBS/ 0.6% agarose. The cells were fed every 3 days by adding 200 μL of RPMI/10% FBS. Colonies were stained with Hoechst33342 and photographed at 10x and 30x magnification after 4 weeks.

**Apoptosis nuclear staining assay**

Apoptotic and necrotic cell death were determined by Hoechst 33342 and propidium iodide (PI) co-staining. After specific treatments, cells were incubated with 10 μM of Hoechst 33342 and 5 μg/ml of PI for 30 min at 37°C. Nuclei condensation and DNA fragmentation of apoptotic cells and PI-positive necrotic cells were visualized and

scored under a fluorescence microscope (Olympus IX51 with DP70; Olympus, Center Valley, PA, USA).

**DNA content analysis**

Cells were seeded at a density of $3\times10^5$ cells/well onto 6-well plate and incubated overnight for cell attachment. After the indicated treatments, cells were trypsinized and fixed in 70% absolute ethanol at -20 °C overnight. After washing with PBS, cells were incubated in propidium iodide solution containing 0.1% Triton-X, 1 μg/ml RNase, and 1 mg/ml propidium iodide at room temperature for 30 min. DNA content was analyzed using flow cytometry (FACSort, Becton Dickinson, Rutherford, NJ) as previously described (Chanvorachote and Pongrakhananon, 2013).

**Migration determination**

Migration was determined by wound healing and Boyden chamber assay as previously described (Luanpitpongt *et al*., 2010). For wound healing assay, cells were seeded at a density of $2\times10^5$ cells/well onto 24-well plate. After the cell monolayer was formed, a micropipette tip was used to scratch cell attachment to generate wound space. The cells were then washed with PBS and replaced with RPMI medium containing indicated concentration of moscatilin. The progress of cell migration into the wound was photographed by inverted microscope (Olympus IX51 with DP70) at indicated time of incubation. The average wound space was calculated from the random field of view and represent as the relative cell migration. Relative cell migration was calculated by dividing the change of wound space of sample by that of the control cells in each experiment. In case of Boyden chamber assay, cells were seeded at a density of $5\times10^4$ cells/well onto upper 24-transwell plate of the transwell filter (8-μM pore) in serum free medium, and incubated with various concentrations of moscatilin. RPMI medium containing 10% FBS was added at lower chamber. Following the incubation, the non-migrate cells in the

upperside membrane were removed by cotton-swab wiping, and cells that migrated to the underside of the membrane were stained with 10 μg/ml Hoechst 33342 for 10 min, visualized and scored under a fluorescence microscope (Olympus IX51 with DP70).

**Invasion assay**

The invasion assay was carried out using 24-transwell chambers as previously described (Luanpitponget *et al*., 2010), which were coated with 50 μl of 0.5% matrigel on the upper surface of chamber overnight at 37 °C in a humidified incubator. Following the incubation, cells were seeded at a density of $5\times10^4$ cells/well onto upper chambers in serum free medium containing various concentrations of moscatilin, and RPMI medium containing 10% FBS was added to the lower chamber. After indicated time, non-invaded cells in the upperside of membrane were removed by cotton-swab wiping. Invaded cells in the underside of membrane were fixed with cold absolute methanol for 10 min, and stained with 10 μg/ml Hoechst 33342 for 10 min. Cells were then visualized, and scored under a fluorescence microscope (Olympus IX51 with DP70).

**Cell morphology characterization**

Cell morphology was investigated by phalloidin-rhodamine and sulforhodamine B staining assay as previously described (Wang *et al*., 2011). Cells were seeded at a density of $10^4$ cells/well onto 96-well plate overnight. Cells were treated with various concentrations of moscatilin for 24 h. Cells were then washed with PBS, fixed with 4% paraformaldehyde in PBS for 10 min at 37℃, permeabilized with 0.1% Triton-X100 in PBS for 4 min, and blocked with 0.2% BSA for 30 min. Cells were then incubated with either 1:100 phalloidin-rhodamine in PBS or 0.4% sulforhodamine B in 1% acetic acid for 15 min, rinsed 3 times with PBS, and mounted with 50% glycerol. Cell morphology was then imaged by fluorescence (Olympus IX51 with DP70). Filopodia protrusion was represented in comparison with control cells.

**Reactive oxygen species detection**

Intracellular ROS were determined using specific ROS detection probe including dichlorofluorescein diacetate ($DCFH_2$-DA; ROS probe), hydroxyphenyl fluorescein (HPF; specific $OH^{\cdot}$ probe), amplex red (specific $H_2O_2$ probe) and dihydroethidium (DHE; specific $O_2^{\cdot -}$ probe) as previously described (Chanvorachote and Pongrakhananon, 2013). After indicated treatments, cells were incubated with either 100 μM of $DCFH_2$-DA, 100 μM of HPF, 10 mM of amplex red or 100 μM of DHE for 30 min at 37°C, after which they were washed, and immediately analyzed for fluorescence intensity using a microplate reader.

**Western blotting**

Cells were seeded at a density of $3\times10^5$ cells/well onto 6-well plates overnight. After specific treatment, cells were washed twice with cold-PBS, and incubated with lysis buffer containing 20 mM Tris-HCl (pH 7.5), 1% Triton X-100, 150 mM sodium chloride, 10% glycerol, 1 mM sodium orthovanadate, 50 mM sodium fluoride, 100 mM phenylmethylsulfonyl fluoride, and protease inhibitor cocktail (Roche Molecular Biochemicals) for 40 min on ice. Cell lysates were collected, and the protein content was determined using the BCA protein assay kit (Pierce Biotechnology, Rockford, IL). Equal amounts of protein from each sample (60 μg) were denatured by heating at 95°C for 5 min with Laemmli loading buffer, and subsequently loaded onto a 10% SDS-polyacrylamide gel for electrophoresis. After separation, proteins were transferred onto 0.45 μM nitrocellulose membranes (Bio-Rad). The transferred membranes were blocked in 5% non-fat dry milk in TBST (25 mM Tris-HCl (pH 7.5), 125 mM NaCl, 0.05% Tween 20) for 1 h, after which it was incubated with a specific primary antibody overnight at 4 °C. Membranes were washed three times with TBST for 10 min and

incubated with Horseradish peroxidase (HRP)-conjugated anti-rabbit or anti-mouse IgG for 2 h at room temperature. After three times-washing with TBST, the immune complexes were detected by enhancement with a chemiluminescent substrate (Supersignal West Pico; Pierce, Rockfore, IL) and quantified using analyst/PC densitometry software (Bio-Rad).

**Statistical Analysis**

All results from four or more independent experiments were presented as the mean ± standard deviation (SD). Statistical differences between the means were analyzed using one-way ANOVA with Turkey *post-hoc* test at a significance level of $p < 0.05$ using SPSS version 19.0.

**Extraction and isolation**

***Dendrobium pulchellum***

Dried, powdered stems of *D. pulchellum* (0.5 kg) were extracted with 95% EtOH (3 x 10 L) at room temperature to give a viscous mass of dried extract (50 g) after evaporation of the solvent. This material was subjected to vacuum-liquid chromatography (VLC) on silica gel (*n*-hexane-EtOAc gradient and MeOH) to give 7 fractions (A-G). Fraction D (1.8 g) was chromatographed on Sephadex LH-20 (MeOH-$CH_2Cl_2$ 1:1) to yield 8 fractions (D-1-D-8). Fraction D-4 (330 mg) was separated by CC over silica gel, eluted with *n*-hexane-EtOAc (7:3) to give 26 fractions. Chrysotobibenzyl (**1**) (54 mg) was obtained from fractions 2-3. Separation of fractions 6-9 (35 mg) by CC (silica gel; *n*-hexane-EtOAc 7:3) gave chrysotoxine (**2**) (11 mg). Fraction D-5 (510 mg) was further separated by CC over silica gel (*n*-hexane-EtOAc gradient) to give crepidatin (**3**) (24 mg) and moscatilin (**4**) (130 mg). Separation of fraction D-7 (60 mg) was performed on silica gel (*n*-hexane-EtOAc gradient) to yield fimbriatone (**5**) (6 mg). Fraction F (4 g) was separated by CC (silica gel; $CH_2Cl_2$-MeOH gradient) and then by CC (silica gel; EtOAc-

MeOH gradient with 1% $H_2O$) to give (-)-shikimic acid (**6**) (145 mg). Fraction G (10 g) was rechromatographed over MCI-gel CHP-20P ($H_2O$-MeOH 1:0 to 1:9) and then by CC (silica gel; EtOAc-MeOH 9:1 with 1% $H_2O$) to afford liriodendrin (**7**) (50 mg).

***Dendrobium ellipsophyllum***

Dried powdered whole plant of *D. ellipsophyllum* (4.8 kg) was extracted with MeOH (3 x 10 L) at room temperature to give a viscous mass of dried extract (400 g) after evaporation of the solvent. This material (200 g) was subjected to vacuum-liquid chromatography (VLC) on silica gel (*n*-hexane-EtOAc gradient) to give 5 fractions (A-E). Fraction D (63 g) was separated by VLC over silica gel, eluted with *n*-hexane-EtOAc gradient to give 7 fractions (D1-D7). Fraction D4 (2.3 g) was separated by column chromatography (CC) (silica gel; *n*-hexane-EtOAc, gradient) and then further purified on Sephadex LH-20 (acetone) to give 5,7-dihydroxy-chromen-4-one (**8**) (4 mg). Fraction D5 (5.4 g) was subjected to medium pressure liquid chromatography (MPLC) over silica gel eluted with *n*-hexane-EtOAc gradient to give 14 fractions (D5A-D5N). Purification of fraction D5D (47 mg) and D5F (828 mg) on Sephadex LH20 (acetone) gave 4,5-Dihydroxy-2,3-dimethoxy-9,10-dihydrophenanthrene (**9**) (9 mg) and moscatilin (**4**) (188 mg), respectively. Fraction D5G (954.3 mg) was separated by CC over silica gel (*n*-hexane-EtOAc, gradient) and further purified on Sephadex LH20 (acetone) to yield 4,4′-dihydroxy-3,5-dimethoxybibenzyl (**10**), 4,5,4′-trihydroxy-3,3′-dimethoxybibenzyl (**11**) and (2*S*)-homoeriodictyol (**12**), respectively. Separation of fraction D5I (1.0 g) by CC (silica gel; *n*-hexane-EtOAc , gradient) gave (2*S*)-eriodictyol (**13**) (364 mg). Fraction D6 (8.6 g) was separated by CC (silica gel; *n*-hexane-EtOAc, gradient) to give 12 fractions (D6A-D6L). Fraction D6I (1.0 g) was subjected to repeated CC over silica gel, eluted with *n*-hexane-EtOAc (gradient) and then further purified on Sephadex LH-20 (acetone)

to furnish chrysoeriol (**14**) (8 mg), phloretic acid (**15**) (18 mg) and luteolin (**16**) (38 mg), respectively.

**Physical and spectral data of isolated compounds**

Chrysotobibenzyl (**1**): Brown amorphous solid; $C_{19}H_{24}O_5$, ESIMS: $[M+H]^+$ *m/z* 333. $^1$H NMR (300 MHz, $CDCl_3$) δ: 2.82 (4H, br s, $H_2$-α, $H_2$-α′), 3.79 (9H, s, MeO-3′, MeO-4′, MeO-5′), 3.81 (3H, s, MeO-3), 3.83 (3H, s, MeO-4), 6.34 (2H, s, H-2′, H-6′), 6.64 (1H, br s, H-2), 6.69 (1H, bd d, *J* = 8.4 Hz, H-6), 6.77 (1H, d, *J* = 8.4 Hz, H-5). $^{13}$C NMR (75 MHz, $CDCl_3$) δ: 37.5 (C-α′), 38.5 (C-α), 55.7 (MeO-3), 55.8 (MeO-4), 55.9 (MeO-3′, MeO-5′), 60.7 (MeO-4′), 105.5 (C-2′, C-6′), 111.3 (C-5), 112.0 (C-2), 120.3 (C-6), 134.2 (C-1), 136.2 (C-4′), 137.4 (C-1′), 147.3 (C-4), 148.7 (C-3), 153.0 (C-3′, C-5′) (Li *et al*., 2011).

Chrysotoxine (**2**): Brown amorphous solid; $C_{18}H_{22}O_5$, ESIMS: $[M+H]^+$ *m/z* 319. $^1$H NMR (300 MHz, $CDCl_3$) δ: 2.79 (4H, br s, $H_2$-α, $H_2$-α′), 3.79 (12H, s, MeO-3, MeO-4, MeO-3′, MeO-5′), 6.33 (2H, s, H-2′, H-6′), 6.63 (1H, br s, H-2), 6.66 (1H, br d, *J* = 8.1 Hz, H-6), 6.75 (1H, d, *J* = 8.1 Hz, H-5). $^{13}$C NMR (75 MHz, $CDCl_3$) δ: 37.4 (C-α′), 37.9 (C-α), 55.5 (MeO-4), 55.8 (MeO-3′, MeO-5′), 56.0 (MeO-6), 105.0 (C-2′, C-6′), 111.1 (C-5), 111.8 (C-2), 120.1 (C-6), 132.5 (C-1′), 132.7 (C-4′), 134.1 (C-1), 146.6 (C-3′, C-5′), 147.0 (C-3), 148.5 (C-4) (Ono *et al*., 1995).

Crepidatin (**3**): Brown amorphous solid; $C_{18}H_{22}O_5$, ESIMS: $[M+H]^+$ *m/z* 319. $^1$H NMR (300 MHz, $CDCl_3$) δ: 2.79 (4H, br s, $H_2$-α, $H_2$-α′), 3.72 (3H, s, MeO-3), 3.75 (6H, s, MeO-3′, MeO-5′), 3.79 (3H, s, MeO-4′), 6.33 (2H, s, H-2′, H-6′), 6.58 (1H, d, *J* = 9.0 Hz, H-2), 6.66 (1H, br d, *J* = 8.1 Hz, H-6), 6.80 (1H, d, *J* = 8.1 Hz, H-5). $^{13}$C NMR (75 MHz, $CDCl_3$) δ: 38.0 (C-α′), 39.0 (C-α), 56.2 (MeO-3), 56.5 (MeO-3′, MeO-5′), 61.2 (MeO-4′), 106.1 (C-2′, C-6′), 111.9 (C-2), 114.8 (C-5), 121.4 (C-6), 133.9 (C-1), 136.7

(C-4′), 138 (C-1′), 144.4 (C-4), 146.9 (C-3), 153.4 (C-3′, C-5′) (Majumder and Chatterjee, 1989).

Moscatilin (**4**): Brown amorphous solid; $C_{17}H_{20}O_5$, ESIMS: $[M+H]^+$ *m/z* 305. $^1$H NMR (300 MHz, $CDCl_3$) δ: 2.80 (4H, br s, $H_2$-α, $H_2$-α′), 3.82 (9H, s, MeO-3, MeO-3′, MeO-5′), 6.34 (2H, s, H-2′, H-6′), 6.60 (1H, br s, H-2), 6.66 (1H, br d, *J* = 8.1 Hz, H-6), 6.82 (1H, d, *J* = 8.1 Hz, H-5). $^{13}$C NMR (75 MHz, $CDCl_3$) δ: 37.8 (C-α′), 38.4 (C-α), 55.8 (MeO-3), 56.2 (MeO-3′, MeO-5′), 105.2 (C-2′, C-6′), 111.2 (C-2), 114.1 (C-5), 121.0 (C-6), 132.8 (C-1), 132.9 (C-1′), 133.6 (C-4′), 143.7 (C-4), 146.2 (C-3), 146.8 (C-3′, C-5′) (Mahumder and Sen, 1987).

Fimbriatone (**5**): Brown amorphous solid; $C_{16}H_{10}O_5$, ESIMS: $[M+H]^+$ *m/z* 283. $^1$H NMR (300 MHz, Acetone-$d_6$) δ: 4.14 (3H, s, MeO-1), 7.09 (1H, d, *J* = 1.8 Hz, H-6), 7.29 (1H, d, *J* = 1.8 Hz, H-8), 7.83 (1H, d, *J* = 9.3 Hz, H-9), 8.05 (1H, d, *J* = 9.3 Hz, H-10), 8.11 (1H, s, H-3). $^{13}$C NMR (75 MHz, Acetone-$d_6$) δ: 61.8 (MeO-1), 103.4 (C-6), 108.0 (C-8), 108.9 (C-4b), 115.2 (C-4), 118.8 (C-3), 121.8 (C-10), 124.0 (C-10a), 124.3 (C-4a), 127.3 (C-9), 132.3 (C-8a), 148.9 (C-2), 149.0 (C-1), 152.1 (C-5), 158.5 (C-7), 161.0 (C=O) (Zhang *et al*., 2008).

(-)-Shikimic acid (**6**): Colorless needles; $C_7H_{10}O_5$, ESIMS: $[M+H]^+$ *m/z* 175. $^1$H NMR (300 MHz, MeOH-$d_4$) δ: 2.19 (1H, dd, *J* = 18.1, 5.5 Hz, H-6*β*), 2.70 (1H, dd, *J* = 18.1, 4.7 Hz, H-6α), 3.68 (1H, m, H-4), 3.98 (1H, dd, *J* = 12.4, 5.5 Hz, H-5), 4.37 (1H, br s, H-3), 6.80 (1H, d, *J* = 1.4 Hz, H-2). $^{13}$C NMR (75 MHz, MeOH-$d_4$) δ: 31.7 (C-6), 67.3 (C-5), 68.4 (C-4), 72.8 (C-3), 130.8 (C-1), 138.7 (C-2), 170.0 (COOH) (Ishimaru *et al*., 1987).

Liriodendrin (**7**): White powder; $C_{34}H_{46}O_{18}$, EIMS: $[M+Na]^+$ 765. $^1$H NMR (300 MHz, DMSO-$d_6$) δ: 3.02-3.08 (12H, overlapped, Glc-H-2′,2′′-H-6′,6′′), 3.08 (2H, m, H-

1, H-5), 3.75 (12H, s, MeO-3′, MeO-5′, MeO-3″, MeO-5″), 3.83 (2H, m, H-4a, H8a), 4.62 (2H, br s, H-2, H-6), 6.64 (4H, br s, H-2, H-2′, H-6, H-6′). $^{13}$C NMR (75 MHz, DMSO-$d_6$) δ: 53.6 (C-1, C-5), 56.5 (MeO-3′, MeO-5′, MeO-3″, MeO-5″), 61.1 (Glc-C-6′, Glc-C-6″), 70.0 (Glc-C-4′, Glc-C-4″), 71.4 (C-4, C-8), 74.2 (Glc-C-2′, Glc-C-2″), 76.5 (Glc-C-3′, Glc-C-3″), 77.2 (Glc-C-5′, Glc-C-5″), 85.1 (C-2, C-6), 102.8 (Glc-C-1′, Glc-C-1″), 104.3 (C-2, C-2′, C-6, C-6′), 133.9 (C-1′, C-1″), 137.2 (C-4′, C-4″), 152.7 (C-3′, C-3″, C-5′, C-5″) (Deyama, 1983).

5,7-Dihydroxy-chromen-4-one (**8**): Colorless needles; $C_9H_6O_4$; ESI-MS *m/z* 179 $[M+H]^+$; $^1$H NMR (300 MHz, acetone-$d_6$) δ: 6.21 (1H, d, *J* = 6.0 Hz, H-3), 6.26 (1H, d, *J* = 2.1 Hz, H-6), 6.39 (1H, d, *J* = 2.1 Hz, H-8), 8.05 (1H, d, *J* = 6.0 Hz, H-2), 12.76 (1H, s, HO-5); $^{13}$C NMR (75 MHz, acetone-$d_6$) δ: 94.7 (C-8), 99.8 (C-6), 106.4 (C-10), 111.5 (C-3), 157.6 (C-2), 159.2 (C-9), 163.4 (C-5), 165.1 (C-7), 182.5 (C-4) (Du *et al*. 2004).

4,5-Dihydroxy-2,3-dimethoxy-9,10-dihydrophenanthrene (**9**): Brown amorphous solid; $C_{16}H_{16}O_4$; ESI-MS *m/z* 273 $[M+H]^+$; $^1$H NMR (300 MHz, $CDCl_3$) δ: 2.72 (4H, m, $H_2$-9, $H_2$-10), 3.93 (3H, s, MeO-2), 3.99 (3H, s, MeO-3), 6.56 (1H, s, H-1), 6.87 (1H, d, *J* = 8.0 Hz, H-8), 6.98 (1H, d, *J* = 8.0 Hz, H-6), 7.16 (1H, t, *J* = 8.0 Hz, H-7); $^{13}$C NMR (75 MHz, $CDCl_3$) δ: 30.9 (C-9, C-10), 55.9 (MeO-2), 61.2 (MeO-3), 105.0 (C-1), 113.1 (C-4a), 118.0 (C-8), 120.0 (C-6), 120.4 (C-4b), 128.0 (C-7), 134.0 (C-3), 136.7 (C-10a), 140.2 (C-8a), 143.7 (C-4), 150.4 (C-2), 153.2 (C-5) (Wollenweber *et al*. 1992).

4,4′-Dihydroxy-3,5-dimethoxybibenzyl (**10**): Brown amorphous solid; $C_{16}H_{18}O_4$; ESI-MS *m/z* 275 $[M+H]^+$; $^1$H NMR (500 MHz, acetone-$d_6$) δ: 2.76 (4H, m, $H_2$-$\alpha$ ,$H_2$-$\alpha'$), 3.76 (6H, s, MeO-3,5), 6.46 (2H,s, H-2,6), 6.72 (2H, d, *J* = 8.5 Hz, H-3′, H-5′), 7.00 (2H,

d, $J$ = 8.5 Hz, H-2′, H-6′); $^{13}$C NMR (125 MHz, acetone-$d_6$) δ: 38.0 (C-$\alpha$′), 39.0 (C-$\alpha$), 56.4 (MeO-3, MeO-5), 106.7 (C-2, C-6), 115.8 (C-3′, C-5′), 130.1 (C-2′, C-6′), 133.1 (C-1), 133.5 (C-1′), 134.9 (C-4), 148.4 (C-3, C-5), 156.3 (C-4′) (Katerere *et al.* 2012).

4,5,4′-Trihydroxy-3,3′-dimethoxybibenzyl (**11**): Brown amorphous solid; $C_{16}H_{18}O_5$; ESI-MS *m/z* 291 $[M+H]^+$; $^1$H NMR (300 MHz, $CDCl_3$) δ: 2.80 (4H, m, $H_2$-$\alpha$ ,$H_2$-$\alpha$′), 3.84 (3H, s, MeO-3), 3.86 (3H, s, MeO-3′), 6.25 (1H, br s, H-2), 6.47 (1H, br s, H-6), 6.65 (1H, br s, H-2′), 6.70 (1H, br d, $J$ = 8.0 Hz, H-6′), 6.85 (1H, d, $J$ = 8.0 Hz, H-5′); $^{13}$C NMR (75 MHz, $CDCl_3$) δ: 37.7 (C-$\alpha$′), 38.2 (C-$\alpha$), 55.9 (MeO-3′), 56.2 (MeO-3), 103.6 (C-2), 108.6 (C-6), 111.2 (C-2′), 114.2 (C-5′), 121.0 (C-6′), 130.5 (C-1), 133.7 (C-4), 133.8 (C-1′), 143.7 (C-5, C-4′), 146.3 (C-3′), 146.7 (C-3) (Sritularak *et al*. 2011b).

(2*S*)-Homoeriodictyol (**12**): Colorless needles; $C_{16}H_{14}O_6$; ESI-MS *m/z* 303 $[M+H]^+$; $[\alpha]_D^{20}$ -18.6 ($c$ = 0.2, MeOH); $^1$H NMR (500 MHz, acetone-$d_6$) δ: 2.72 (1H, dd, $J$ = 17.0, 3.0Hz, H-3$_{cis}$), 3.19 (1H, dd, $J$ = 17.0, 13.0 Hz, H-3$_{trans}$), 3.87 (3H, s, MeO-3′), 5.41 (1H, dd, $J$ = 13.0, 3.0 Hz, H-2), 5.94 (1H, d, $J$ = 2.5 Hz, H-6), 5.96 (1H, d, $J$ = 2.5 Hz, H-8), 6.86 (1H, d, $J$ = 8.0 Hz, H-5′), 6.98 (1H, dd, $J$ = 8.0, 2.0 Hz, H-6′), 7.17 (1H, d, $J$ = 2.0 Hz, H-2′), 12.17 (1H, s, HO-5); $^{13}$C NMR (125 MHz, acetone-$d_6$) δ: 43.5 (C-3), 56.2 (MeO-3′), 80.1 (C-2), 95.8 (C-8), 96.7 (C-6), 103.1 (C-10), 111.1 (C-2′), 115.6 (C-5′), 120.4 (C-6′), 131.2 (C-1′), 147.8 (C-4′), 148.3 (C-3′), 164.3 (C-9), 165.2 (C-5), 167.3 (C-7), 197.2 (C-4) (Liu *et al*. 1992).

(2*S*)-Eriodictyol (**13**): Colorless needles; $C_{15}H_{12}O_6$; ESI-MS *m/z* 289 $[M+H]^+$; $[\alpha]_D^{20}$ -18.7 ($c$ = 0.2, MeOH); $^1$H NMR (500 MHz, acetone-$d_6$) δ: 2.72 (1H, dd, $J$ = 17.0, 3.0

Hz, H-3$_{cis}$), 3.11 (1H, dd, *J* = 17.0, 12.5 Hz, H-3$_{trans}$), 5.37 (1H, dd, *J* = 12.5, 3.0 Hz, H-2), 5.93 (1H, d, *J* = 2.0 Hz, H-6), 5.95 (1H, d, *J* = 2.0 Hz, H-8), 6.86 (2H, d, *J* = 1.5 Hz, H-5′, H-6′), 7.02 (1H, d, *J* = 1.5 Hz, H-2′), 12.16 (1H, s, HO-5); $^{13}$C NMR (125 MHz, acetone-$d_6$) δ: 43.4 (C-3), 79.9 (C-2), 95.8 (C-8), 96.7 (C-6), 103.1 (C-10), 114.6 (C-2′), 115.9 (C-5′), 119.2 (C-6′), 131.5 (C-1′), 145.9 (C-3′), 146.3 (C-4′), 164.2 (C-5), 165.2 (C-9), 167.2 (C-7), 197.1 (C-4) (Encarnación *et al*. 1999).

Chrysoeriol (**14**): Yellow powder; $C_{16}H_{12}O_6$; ESI-MS *m/z* 301 $[M+H]^+$; $^1$H NMR (500 MHz, acetone-$d_6$) δ: 3.98 (3H, s, MeO-3′), 6.24 (1H, d, *J* = 2.0 Hz, H-6), 6.54 (1H, d, *J* = 2.0 Hz, H-8), 6.69 (1H, s, H-3), 7.00 (1H, d, *J* = 8.4 Hz, H-5′), 7.59 (1H, dd, *J* = 8.4, 2.0 Hz, H-6′), 7.63 (1H, d, J = 2.0 Hz, H-2′), 13.01 (1H, s, HO-5); $^{13}$C NMR (125 MHz, acetone-$d_6$) δ: 56.5 (MeO-3′), 94.7 (C-8), 99.7 (C-6), 104.4 (C-3), 105.1 (C-10), 110.5 (C-2′), 116.3 (C-5′), 121.3 (C-6′), 123.6 (C-1′), 148.8 (C-3′), 151.4 (C-4′), 157.8 (C-9), 159.0 (C-5), 163.3 (C-2), 164.9 (C-7), 183.1 (C-4) (Park *et al*. 2007a).

Phloretic acid (**15**): Brown amorphous solid; $C_9H_{10}O_3$; ESI-MS *m/z* 167 $[M+H]^+$; $^1$H NMR (300 MHz, acetone-$d_6$) δ: 2.53 (2H, t, *J* = 7.8 Hz, $H_2$-8), 2.79 (2H, t, *J* = 7.8 Hz, $H_2$-7), 6.74 (2H, d, *J* = 8.1 Hz, H-3, H-5), 7.05 (2H, d, *J* = 8.1 Hz, H-2, H-6); $^{13}$C NMR (75 MHz, acetone-$d_6$) δ: 30.7 (C-7), 36.3 (C-8), 115.8 (C-3, C-5), 130.1 (C-2, C-6), 132.5 (C-1), 156.4 (C-4), 173.9 (C-9) (Owen *et al*. 2003).

Luteolin (**16**): Yellow powder; $C_{15}H_{10}O_6$; ESI-MS *m/z* 287 $[M+H]^+$; $^1$H NMR (500 MHz, acetone-$d_6$) δ: 6.24 (1H, d, *J* = 2.0 Hz, H-6), 6.51 (1H, d, *J* = 2.0 Hz, H-8), 6.57 (1H, s, H-3), 7.00 (1H, d, *J* = 8.4 Hz, H-5′), 7.47 (1H, dd, *J* = 8.4, 2.1 Hz, H-6′), 7.49 (1H, d, *J* = 2.1 Hz, H-2′); $^{13}$C NMR (125 MHz, acetone-$d_6$) δ: 94.6 (C-8), 99.7 (C-6),

104.2 (C-3), 105.3 (C-10), 114.1 (C-2′), 116.6 (C-5′), 120.1 (C-6′), 123.8 (C-1′), 146.4 (C-3′), 150.0 (C-4′), 158.8 (C-9), 163.4 (C-5), 164.8 (C-2), 165.1 (C-7), 183.0 (C-4) (Park *et al*, 2007b).

## RESULTS AND DISCUSSION

### 1. Search for cytotoxic agents from *Dendrobium* spp.

In this study, methanolic extract prepared from eight *Dendrobium* spp., which included *D. ellipsophyllum*, *D. venustum*, *D. lindleyi*, *D. brymerianum*, *D. williamsonii*, *D. densiflorum*, *D. pulchellum* and *D. signatum* were examined for cytotoxicity against human lung cancer cell lines. At 100 μg/ml, two plant extracts (*D. pullchellum* and *D. ellipsophyllum*) exhibited 80% inhibition whereas other plant extracts were devoid of activity. Therefore, these two plants were selected for further investigation for the cytotoxic principles.

### 1.1 Cytotoxic and anti-metastatic activities of compounds from *D. pulchellum*

*Dendrobium pulchellum* Roxb., locally known as "Ueang kham ta khwai", is a plant distributed throughout Thailand. In this study, a MeOH extract prepared from the aerial parts of this plant was found to possess cytotoxic effects against human lung cancer cells. Subsequent chemical investigation of the extract resulted in the isolation of four known bibenzyls, named chrysotobibenzyl (**1**) (Li *et al*., 2011), chrysotoxine (**2**) (Ono *et al*., 1995), crepidatin (**3**) (Majumder and Chatterjee, 1989) and moscatilin (**4**) (Mahumder and Sen, 1987), together with fimbriatone (**5**) (Zhang *et al*., 2008), (-)-shikimic acid (**6**) (Ishimaru et al., 1987) and liriodendrin (**7**) (Deyama, 1983) (Figure 2). Identification of these isolates was carried out by comparison of their NMR and MS data

with reported values. This study is the first report on the chemical composition of *D. pulchellum*. Each of these isolates was then studied for its anti-metastasis potential.

To evaluate their cytotoxic potential, the isolated compounds (**1**-**7**) were examined for cytotoxicity against human lung cancer H23 cells. Each compound was tested at various concentrations for 24 h, and cell viability was determined using the XTT assay. It was found that treatment of the cancer cells with these compounds resulted in a decrease in cell viability in a dose-dependent manner, and the $IC_{50}$ value of each compound was obtained, as shown in Table 1. Our results are consistent with previous findings that moscatilin (**4**) possessed strong cytotoxic activity against several types of cancer cells (Ho and Chen, 2003; Chen *et al*., 2008; Tsi *et al*., 2010). In our study, moscatilin (**4**) at the concentration of approximately 33.4 μM could induce 50% reduction in H23 cell viability, while chrysotobibenzyl (**1**), chrysotoxine (**2**), and crepidatin (**3**) showed recognizable cytotoxicity. The remaining compounds, fimbriatone (**5**), (-)-shikimic acid (**6**), and liriodendrin (**7**) exhibited relatively weak activity, with $IC_{50}$ values of more than 300 μM.

**Table 1**: $IC_{50}$ values for cytotoxicity of isolated compounds from *D. pulchellum* on human lung cancer H23 cells

| **Compounds** | **$IC_{50}$ (μM)** |
|---|---|
| Chrysotobibenzyl (**1**) | 252.14 ± 12.21 |
| Chrysotoxine (**2**) | 198.38 ± 9.28 |
| Crepidatin (**3**) | 157.77 ± 11.21 |
| Moscatilin (**4**) | 33.41 ± 5.36 |
| Fimbriatone (**5**) | > 300 |
| (-)-Shikimic acid (**6**) | > 300 |
| Liriodendrin (**7**) | > 300 |

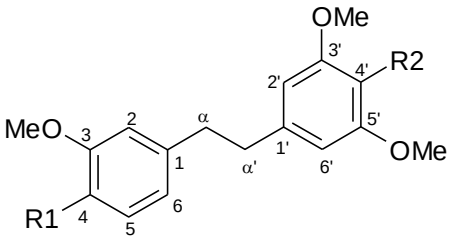


| | $R_1$ | $R_2$ |
|---|---|---|
| **1** | OMe | OMe |
| **2** | OMe | OH |
| **3** | OH | OMe |
| **4** | OH | OH |

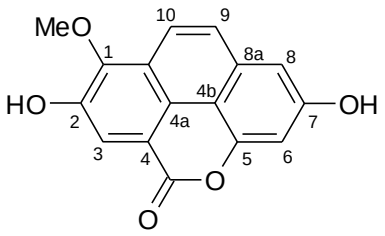


**5**

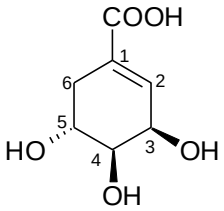


**6**

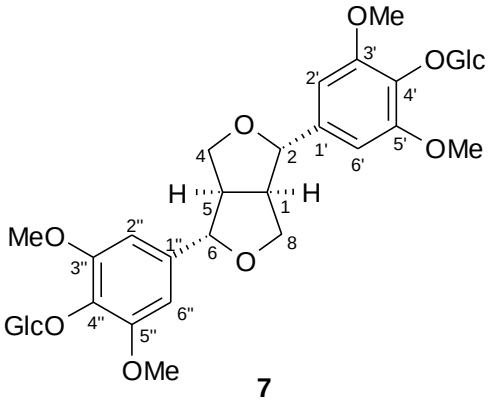


**7**

**Figure 2** Structures of isolated compounds from *Dendrobium pulchellum*

Since the anoikis sensitizing activity and anti-metastasic potential of compounds **1-4** had not been investigated, this study thus attempted to examine their ability in attenuating growth in an anchorage-independent condition, as well as in facilitating anoikis of lung cancer cells. Anchorage-independent growth and anoikis resistance have long been known to be key determining factors for success in metastasis of cancers (Hanahan and Weinberg, 2000; Shanmugathasan and Jothy, 2000; Mori *et al*., 2009). Previously, we reported the anti-metastasic activity of renieramycin M, a marine tetrahydroisoquinoline alkaloid, against lung cancer H460 cells (Halim *et al*., 2011). In this study, chrysotobibenzyl (**1**), chrysotoxine (**2**), crepidatin (**3**), and moscatilin (**4**), at non-cytotoxic concentrations, were tested in detached condition assays. Figure 3 indicates that treatment of the cells with compounds **1-4** at the concentrations of 0, 0.5, and 1 μM caused significant enhancing effect on cell anoikis in a concentration-dependent manner. Moscatilin (**4**) exhibited the highest anoikis sensitizing activity, whereas chrysotoxine (**2**) and crepidatin (**3**) had relatively similar, but less activity. Chrysotobibenzyl (**1**) displayed no anoikis sensitizing effect on these cells, and this correlates with its low cytotoxicity. However, it should be noted that chrysotoxine (**2**) and crepidatin (**3**) had slightly different $IC_{50}$ values, and their effects on cell anokis were quite similar. Furthermore, it can be seen from Figures 4-7 that these four compounds produced an inhibitory effect on cancer cell growth in anchorage-independent conditions. It is very interesting to note herein that although moscatilin (**4**) exhibited higher cytotoxic and anoikis sensitizing activities, its ability in attenuating cancer cell growth in soft agar was comparable with that of chrysotoxine (**2**) and crepidatin (**3**). As expected, chrysotobibenzyl (**1**) exhibited weak activity in inhibiting growth in the detached condition (Figure 4).

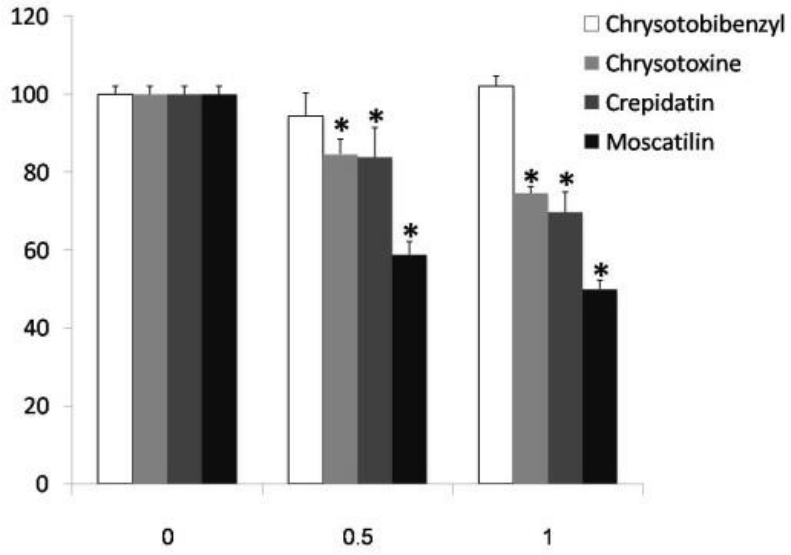


**Figure 3**. Anoikis activity of indicated compounds as assessed by anoikis assay. Cells were exposed to chrysotobibenzyl (**1**), chrysotoxine (**2**), crepidatin (**3**), or moscatilin (**4**) in detached condition for 24 h, and cell viability was determined by XTT assay. Values are means of triplicate samples ± SD. *, $P<0.05$ versus untreated control.

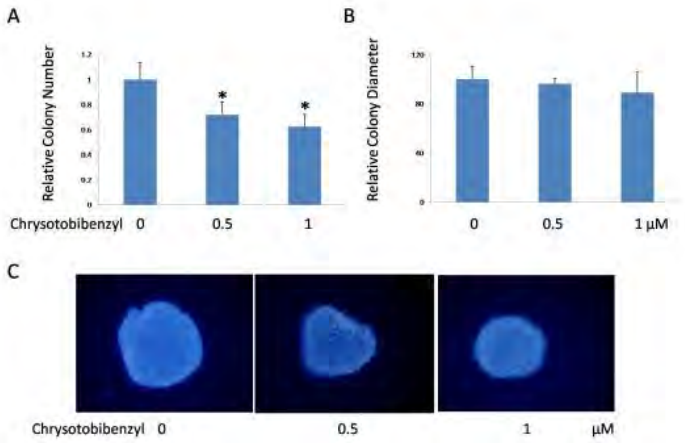


**Figure 4**. Effects of chrysotobibenzyl (**1**) on anchorage-independent growth of H23 cells. H23 cells were detached and left untreated (control) or treated with 0-1 μM chrysotobibenzyl under a suspended condition in soft agar containing RPMI, 10% FBS, and 0.33% agarose, as described in Experimental. Representative fields from three independent experiments were photographed. (A) the relative cell colony number and (B) relative cell colony diameter were determined by using an image analyzer. Values are mean ± SD (n=3). *$p < 0.05$ versus control. (C) Fluorescence microscopy of Hoechst staining of cell colony.

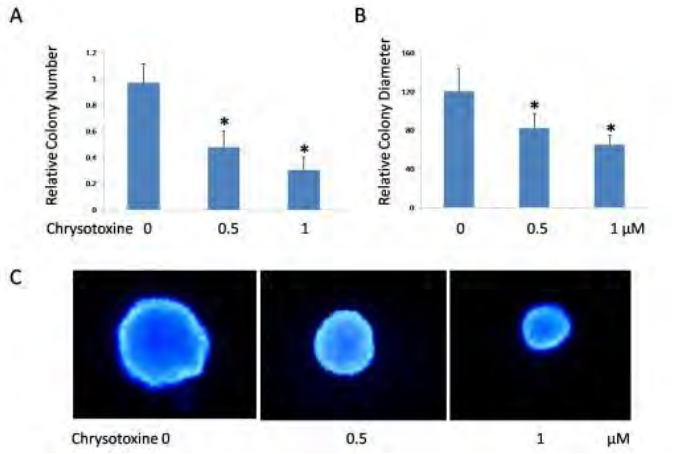


**Figure 5.** Effects of chrysotoxine (**2**) on anchorage-independent growth of H23 cells. H23 cells were detached and left untreated (control) or treated with 0-1 μM chrysotoxine under a suspending condition in soft agar containing RPMI, 10% FBS, and 0.33% agarose as described in Experimental. Representative fields from three independent experiments were photographed. (A) the relative cell colony number and (B) relative cell colony diameter were determined by using image analyzer. Values are mean ± SD (n=3). **p* < 0.05 versus control. (C) Fluorescence microscopy of Hoechst staining of cell colony.

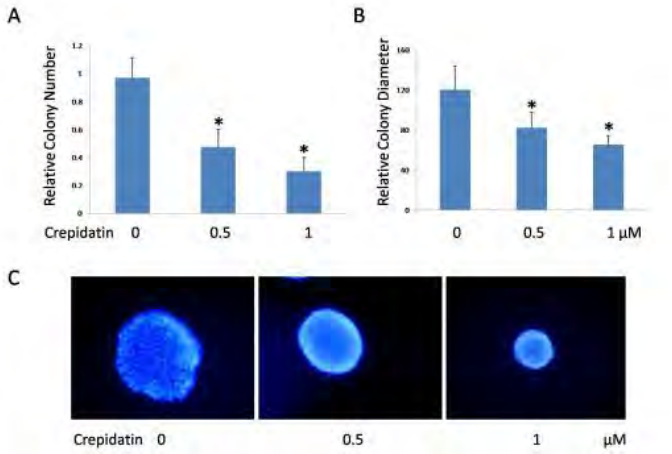


**Figure 6.** Effects of crepidatin (**3**) on anchorage-independent growth of H23 cells. H23 cells were detached and left untreated (control) or treated with 0-1 μM crepidatin under a suspending condition in soft agar containing RPMI, 10% FBS, and 0.33% agarose, as described in Experimental. Representative fields from three independent experiments were photographed. (A) the relative cell colony number and (B) relative cell colony diameter were determined by using an image analyzer. Values are mean ± SD (n=3). **p* < 0.05 versus control. (C) Fluorescence microscopy of Hoechst staining of cell colony.

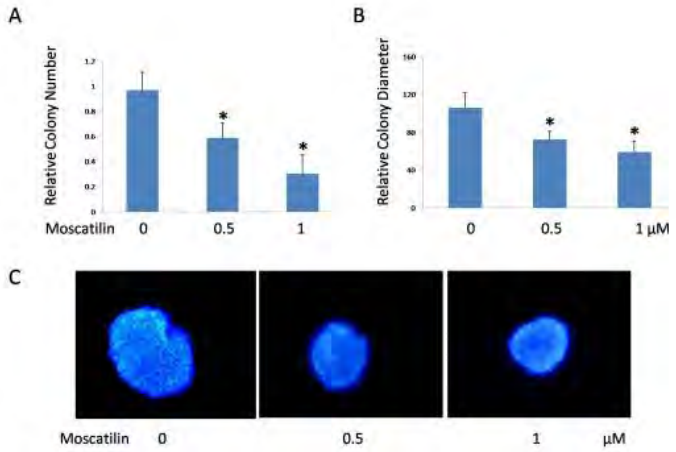


**Figure 7**. Effects of moscatilin (**4**) on anchorage-independent growth of H23 cells. H23 cells were detached and left untreated (control) or treated with 0-1 µM moscatilin under a suspending condition in soft agar containing RPMI, 10% FBS, and 0.33% agarose, as described in Experimental. Representative fields from three independent experiments were photographed. (A) the relative cell colony number and (B) relative cell colony diameter were determined by using an image analyzer. Values are mean ± SD (n=3). *$p$ < 0.05 versus control. (C) Fluorescence microscopy of Hoechst staining of cell colony.

In summary, the present study provides novel data on the anti-metastasic potential of bibenzyls isolated from *D. pulchellum*. Although further investigations, as well as determination of their mechanism of actions are necessary, these polyphenols offer a new approach for cancer drug research.

### 1.2 Cytotoxic and anti-metastatic activities of compounds from *D. ellipsophyllum*

*D. ellipsophyllum* Tang & Wang, locally known as "Ueang thong", is a plant distributed throughout Thailand. Phytochemical investigation of the MeOH extract of the whole plant of *D. ellipsophyllum* led to the isolation of 10 phenolic compounds (Figure 8). The structures of the isolates were determined through analysis of their spectroscopic data in comparison with reported values, and they were identified as 5,7-dihydroxy-chromen-4-one (**8**) (Du *et al.* 2004), 4,5-dihydroxy-2,3-dimethoxy-9,10-dihydrophenanthrene (**9**) (Wollenweber *et al*. 1992), moscatilin (**4**) (Majumder and Sen

1987), 4,4′-dihydroxy-3,5-dimethoxybibenzyl (**10**) (Katerere *et al*. 2012), 4,5,4′-trihydroxy-3,3′-dimethoxybibenzyl (**11**) (Sritularak *et al*. 2011b), (2*S*)-homoeriodictyol (**12**) (Liu *et al*. 1992), (2*S*)-eriodictyol (**13**) (Encarnación *et al*. 1999), chrysoeriol (**14**) (Park *et al.* 2007a), phloretic acid (**15**) (Owen *et al*. 2003) and luteolin (**16**) (Park *et al*, 2007b). This study is the first report on the chemical composition of *D. ellipsophyllum*. Each of these isolates was then investigated for its cytotoxicity. The cytotoxic compounds were evaluated for apoptosis induction and anti-metastatic effects.

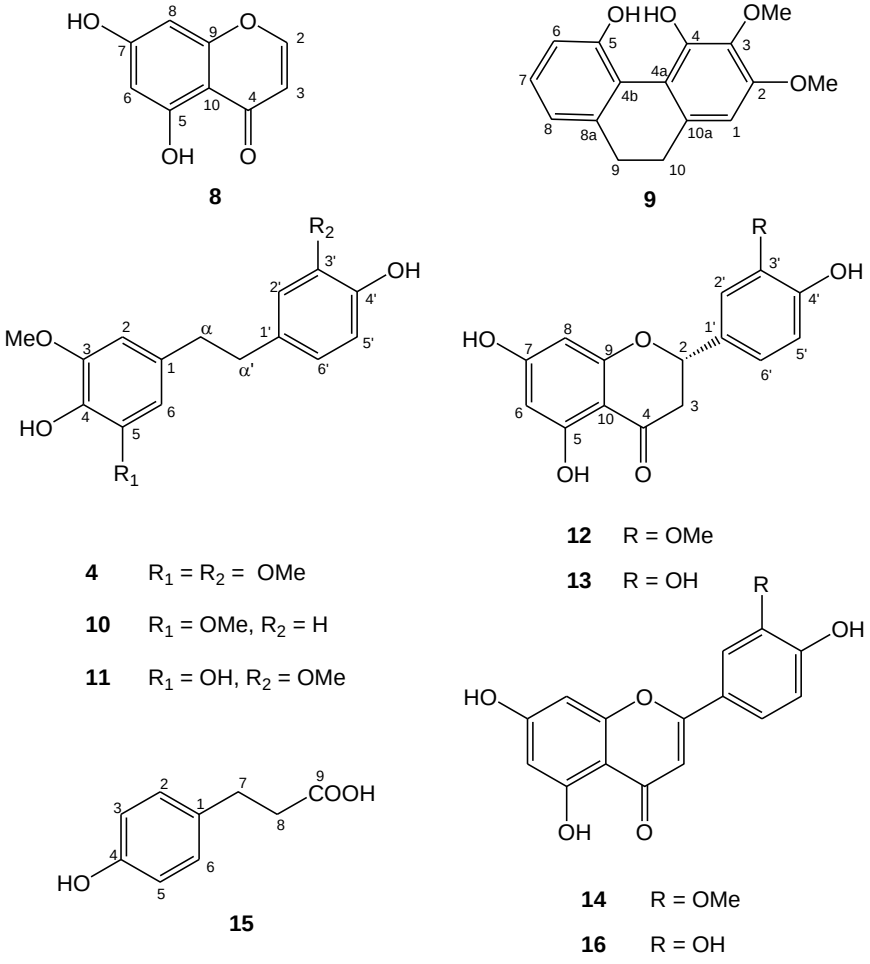


**Figure 8** Structures of compounds from *Dendrobium ellipsophyllum*

*Cytotoxicity on lung cancer cells*

The compounds isolated from *D. ellipsophyllum* were further investigated for the cytotoxicity on human lung cancer cells. Subconfluent (80-90%) monolayer H292 cells were treated with these compounds at the concentrations of 100 μM for 24 h, and the cell viability was evaluated by XTT assay. Two bibenzyls, namely, 4,4′-dihydroxy-3,5-dimethoxybibenzyl (**10**) and 4,5,4′-trihydroxy-3,3′-dimethoxybibenzyl (**11**), and two flavonoids, namely, chrysoeriol (**14**) and luteolin (**16**) exhibited appreciable cytotoxic effect against H292 cells. The $IC_{50}$ of all compounds was determined, and is shown in Table 2. It is worth noting that compound **11** exhibited the strongest anti-cancer activity with $IC_{50}$ 96.59 μM. Because the major concern for the treatment of lung cancer besides cancer metastasis is the possibility of the cells being resistant to drugs, we aimed to elucidate the possible dual anti-cancer and anti-metastasis effects of the compounds. As we were interested in the compounds that have both actions, the compounds possessing potent anti-cancer activity with $IC_{50}$ value less than 250 μM were selected for further elucidation.

*Apoptosis induction effect of the compounds*

The main mechanism of action of current anti-cancer drugs is to induce apoptosis of the cancer cells (Zhang *et al*. 2012). Apoptosis machinery is a critical mechanism of the body to eliminate the harmful cells. The cell will die from the mechanism inside and cause no effect to the surrounded cells (Reed, 2000). Unlike apoptosis, necrosis or accidental cell death is mediated by strong toxic or trauma that directly lyses cells. Necrosis will release cellular substances to the extracellular environment, resulting in the activation of immune system as well as inflammation (Golstein and Kroemer, 2007). Together, apoptosis mode of action was accepted as an important and safe way to

eliminate cancer cells in human. Therefore, the apoptosis induction activity of the compounds was demonstrated in the present study. Lung cancer cells were exposed to compounds **10**, **11**, **14**, and **16** for 24 h, and apoptosis as well as necrosis cell death were determined by Hoechst33342 and PI co-staining assay. Figure 9 shows that all compounds at the concentration of 100 and 200 μM significantly induced the apoptosis of the cells as indicated by an increase in cell possessing condensed and/or fragmented nuclei. The results are consistent with the above finding that compound **11** has the highest anti-cancer activity.

*Anoikis sensitizing activity*

Because the anoikis sensitizing activity and anti-metastasic potential of compounds 4,4′-dihydroxy-3,5-dimethoxybibenzyl (**10)**, 4,5,4′-trihydroxy-3,3′-dimethoxybibenzyl (**11**) and chrysoeriol (**14**) have not been investigated, this study attempted to examine their ability at enhancing anoikis response of the metastatic lung cancer cells. Although anti-metastatic effect of luteolin (**16**) has been reported, there is no record on its anoikis sensitizing activity. Anti-metastatic property of luteolin was due to its ability to inhibit Raf and phosphatidylinositol 3-kinase (PI3K) activities (Kim *et al*. 2013). Anoikis resistance has been recognized as an important factor for success in metastasis (Hanahan and Weinberg 2000; Shanmugathasan and Jothy 2000; Mori *et al*. 2009). We have first investigated for the non-cytotoxic concentrations of the compounds. The results indicated that all compounds at the concentration of 1-5 μM had no effect on cell viability of the adhered H292 cells (data not shown). The cells were then treated with 0-5 μM in detached condition and cell viability over time was evaluated as described in the Procedures. Interestingly, our results indicated that the metastatic lung cancer cells had high anoikis resistance (Figure 10) as indicated by approximately 60 % of the cells

survival after 24-h detachment. Importantly, the treatment of the cells with compounds at these non-toxic concentrations significantly enhanced cell anoikis. These results suggested the possible anoikis sensitizing effect of the compounds. It is interesting that compound **11**, possessing highest cytotoxic activity, also had the fastest action in sensitizing the cells to anoikis. A significant effect was detected as early as 6 h of treatment with compound **11** was comparable to that of other tested compounds.

**Table 2**. $IC_{50}$ values for cytotoxicity of isolated compounds from *D. ellipsophyllum* on human lung cancer H292 cells.

| **Compounds** | **$IC_{50}$ (μM)** |
|---|---|
| 5,7-Dihydroxy-chromen-4-one (**8**) | > 250 |
| 4,5-Dihydroxy-2,3-dimethoxy-9,10-dihydrophenanthrene (**9**) | > 250 |
| Moscatilin (**4**) | 226.09 ± 5.67 |
| 4,4′-Dihydroxy-3,5-dimethoxybibenzyl (**10**) | 197.74 ± 0.78 |
| 4,5,4′-Trihydroxy-3,3′-dimethoxybibenzyl (**11**) | 96.56 ± 0.22 |
| (2*S*)-Homoeriodictyol (**12**) | > 250 |
| (2*S*)-Eriodictyol (**13**) | > 250 |
| Chrysoeriol (**14**) | 217.74 ± 3.08 |
| Phloretic acid (**15**) | > 250 |
| Luteolin (**16**) | 202.57 ± 0.43 |

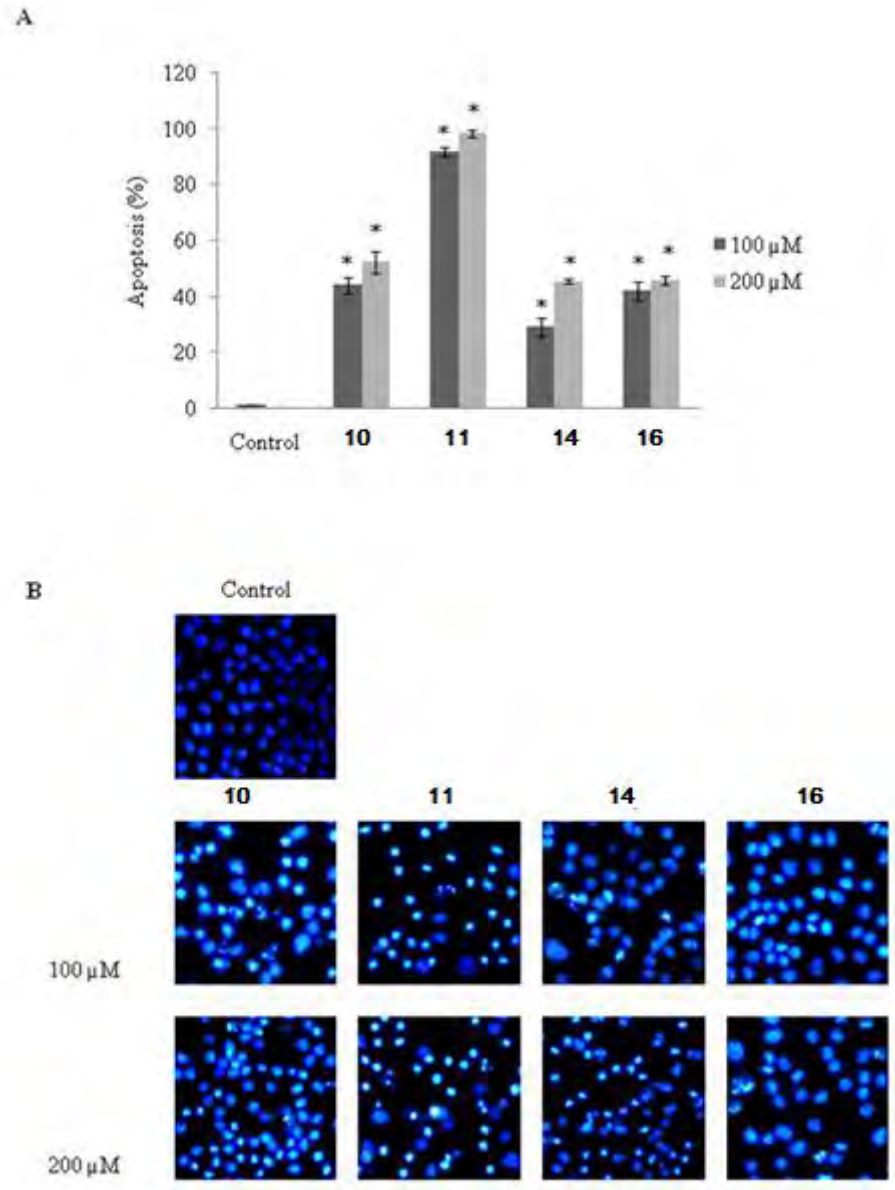


**Figure 9** (A) Percentage of cell apoptosis of compounds **10**, **11**, **14** and **16** was obtained from Hoechst 33342/propidium iodide (PI) assays. Data represent the means ± SD (n =3). * $P < 0.05$ versus nontreated control cells. (B) Morphology of apoptotic nuclei stained with Hoechst 33342 and propidium iodide.

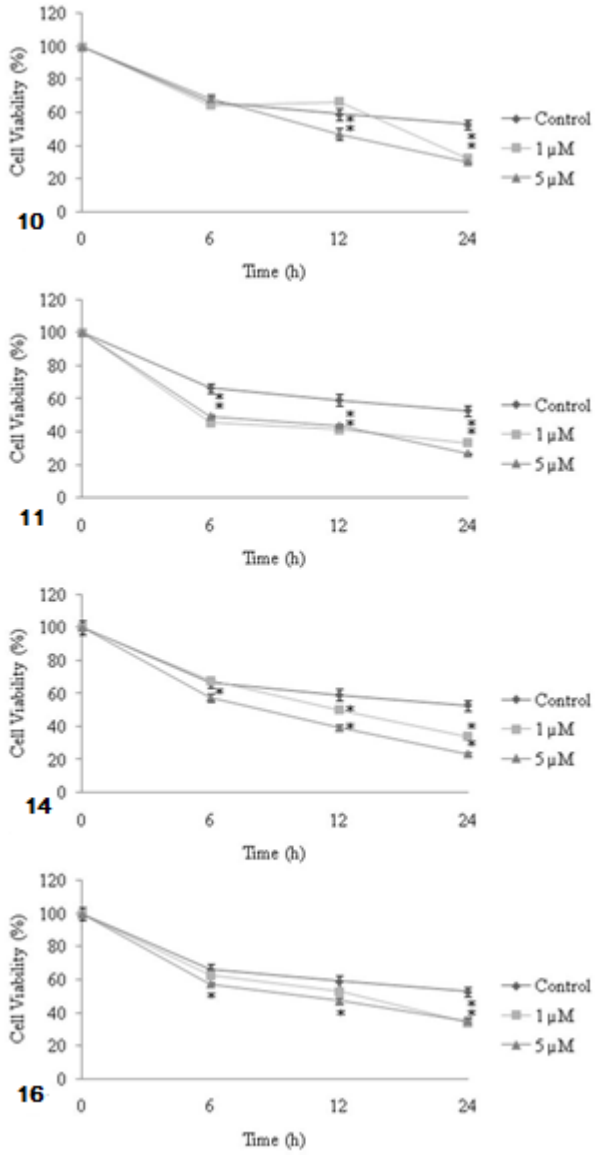


**Figure 10** Anoikis activity of compounds **10**, **11**, **14** and **16** as assessed by anoikis assay. The cells were exposed with various concentrations of each compound (0-5 μM) and the cell viability was determined by XTT assay at the indicated time. Data represent the mean ± SD (n =3). * $P < 0.05$ versus nontreated control cells.

In summary, our results demonstrated the possible anti-cancer and anti-metastatic effects of bibenzyls and flavonoids isolated from *D. ellipsophyllum* that may encourage further investigation and development of these compounds for use cancer treatment.

**2. Evaluation for mechanism of action of moscatilin against lung cancer cells**

Lung cancer incidences have continued to increase worldwide (Siegel *et al*., 2012). More than 90% of lung cancer patients have died from metastasis because of late diagnosis after metastasis was established (Ray and Jablons, 2009). Treatment of metastasis lung cancer often fails due to the acquisition of chemotherapeutic resistance, and the fact that cancer metastasis is still remaining even the tumor are removed by a surgery (Shanker *et al*., 2010). Recently, a number of researches have been conducted to explore potential agents for treatment of cancer metastasis. Cancer metastasis consists of multistep events facilitating the establishment of secondary tumor, in which migration and invasion play critical steps during metastasis involving the elongation of filopodia, cell contraction and gliding, and cell protrusion and reattachment to extracellular matrix (Fidler, 2002; Mattila and Lappalainen, 2008).

Aberrant generation of cellular ROS was tightly associated with several metastasis cancers such as lung, ovary, colon and prostate cancers (Luanpitpong *et al*, 2010; Lei *et al*., 2011). Reactive oxygen species (ROS) such as superoxide anion ($O_2^{-\bullet}$), hydrogen peroxide ($H_2O_2$) and hydroxyl radical ($OH^{\bullet}$) served as important regulators of various physiological pathways during cancer metastasis including angiogenesis, cancer motility and invasiveness (Luanpitpong *et al*, 2010; Hung *et al*., 2012). Scientific evidence also showed that cancer migration and invasion are obviously regulated by reactive oxygen species (ROS) (Luanpitpong *et al*, 2010; Hung *et al*., 2012). It was demonstrated that treatment with antioxidant such as ascorbic acid caused a reduction in cancer motility and invasion (Wei *et al*., 2003), conversely the addition of exogenous ROS enhances these activities (Storz, 2005).

Moscatilin (4,4′-dihydroxy-3,3′,5′-trimethoxybibenzyl) is a bibenzyl derivative isolated from Thai orchid *Dendrobium pulchellum* (Orchidaceae), which is known as "Ueang chang nao" in Thai (Figure 11). Moscatilin was reported to have various pharmacological properties such as anti-inflammatory (Liu *et al*., 2009), antioxidant (Zhang *et al*., 2007) and antiplatelet aggregation (Chen *et al*., 1994). Recently, it has shown anticancer activity against many kinds of cancers for example, induction of cell cycle G2-M arrest (Ho and Chen, 2003; Chen *et al*., 2008) and cell apoptosis involving its antioxidant effect (Zhang *et al*, 2007; Chen *et al*., 2008). In present study, we investigated that the administration of moscatilin attenuates migration and invasion in lung cancer cells. Its negative regulator is associated with the ability of compound to suppress endogenous ROS generation and consequently inhibits FAK and Akt activation-mediating cancer motility and invasiveness. Our finding reveals the novel mechanism of moscatilin on the regulation of cancer migration and invasion, which could be advantage in development of this compound for cancer therapy.

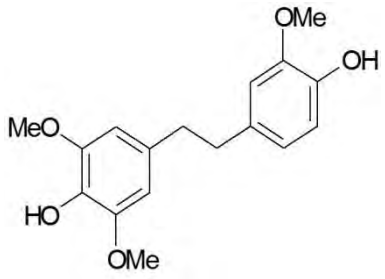


**Figure 11.** Chemical structure of moscatilin

## Results

*Cytotoxicity of moscatilin to H23 cells*

To investigate the inhibitory effect of moscatilin on cancer migration and invasion, prerequisite information regarding its cytotoxicity is crucial. Human lung H23 cells were treated with various concentrations of moscatilin (0-5 μM) for 0-48 h, and cell viability

was examined by MTT assay. Figures 12A and B show that a significant cytotoxic effect of moscatilin was appeared at the concentration of 5 μM at 24 h, with approximatly 70% of cells remaining viable, while the concentrations of such a substance less than 1 μM show non-toxic effect in both dose and time studies. Hoechst33342/PI assay also confirmed that apoptosis and necrotic cell death were not found significantly in response to 0-1 μM moscatilin, whereas apoptotic nuclei were appeared in the cells treated with 5 μM of moscatilin, similar with the data obtained from Annexin-V Staining Assay (Fig. 12C). Consistent with the above findings, DNA content analysis revealed that treatment with 0-1 μM moscatilin caused no detectable change in the percentage of cells in each phase of cell cycle, compared with non-treated control (Fig. 12D). This result suggests that lower doses of moscatilin (0-1 μM) caused neither toxic nor proliferative effects on lung cancer H23 cells.

*Effect of moscatilin on H23 cells migration*

The negative regulatory role of moscatilin on lung cancer migration was investigated by wound healing and Boyden chamber assays. Figures 13A and C show that treatment of the cells with non-toxic doses of moscatilin (0-1 μM) inhibited migration of the cells across the wound space in a dose-dependent manner, of which approximately 0.75- and 0.55-fold of relative migration level were found in cells treated with 0.5 and 1 μM, respectively, compared with nontreated control cells. In addition, moscatilin also causes antimigrative effect in a time-dependent study (Fig. 13B and C). Boyden chamber assay supported our finding that the migrating cells on lower side of membrane were decreased gradually in dose- and time-dependent manners (Fig. 13D, E and F). These results suggest the promising role of moscatilin on regulation of lung cancer migration.

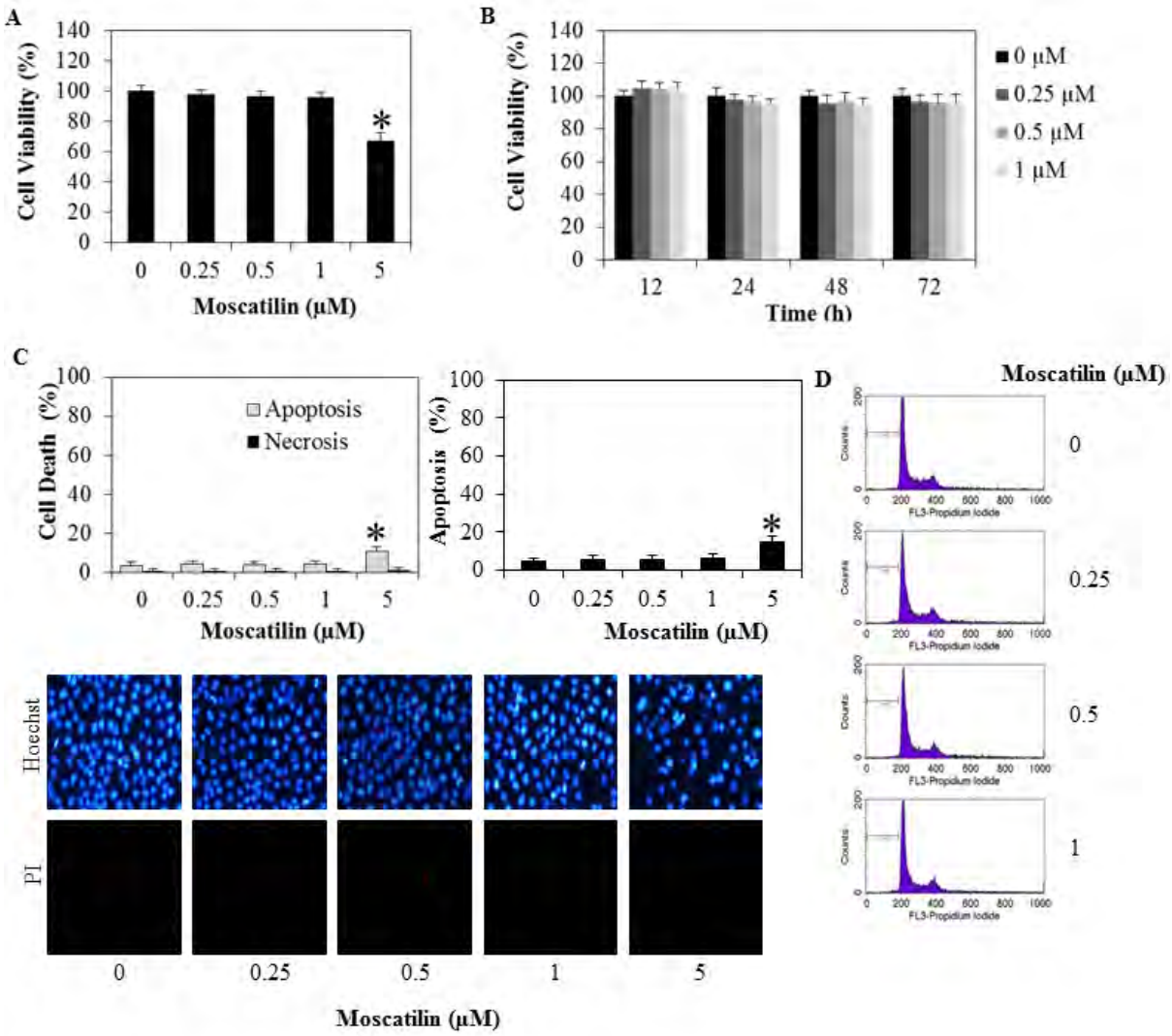


**Figure 12.** Cytotoxicity of moscatilin on human lung H23 cells. (A) Cells were treated with various concentrations of moscatilin (0-5 μM) for 24 h. (B) Cells were treated with moscatilin (0-1 μM) for various times (0-72 h). Cytotoxicity was determined by 3-(4,5-dimethly-thiazol-2-yl)-2,5-diphenyl tetrazolium bromide (MTT) assay. (C) After indicated treatment for 24 h, mode of cell death was examined by Hoechst33342/PI co-staining assay and Annexin-V Staining Assay. (D) Cellular apoptosis was determined by DNA content analysis using flow cytometry. Data represent the means ± SD (n=4). **P* < 0.05 vs. non-treated control cells.

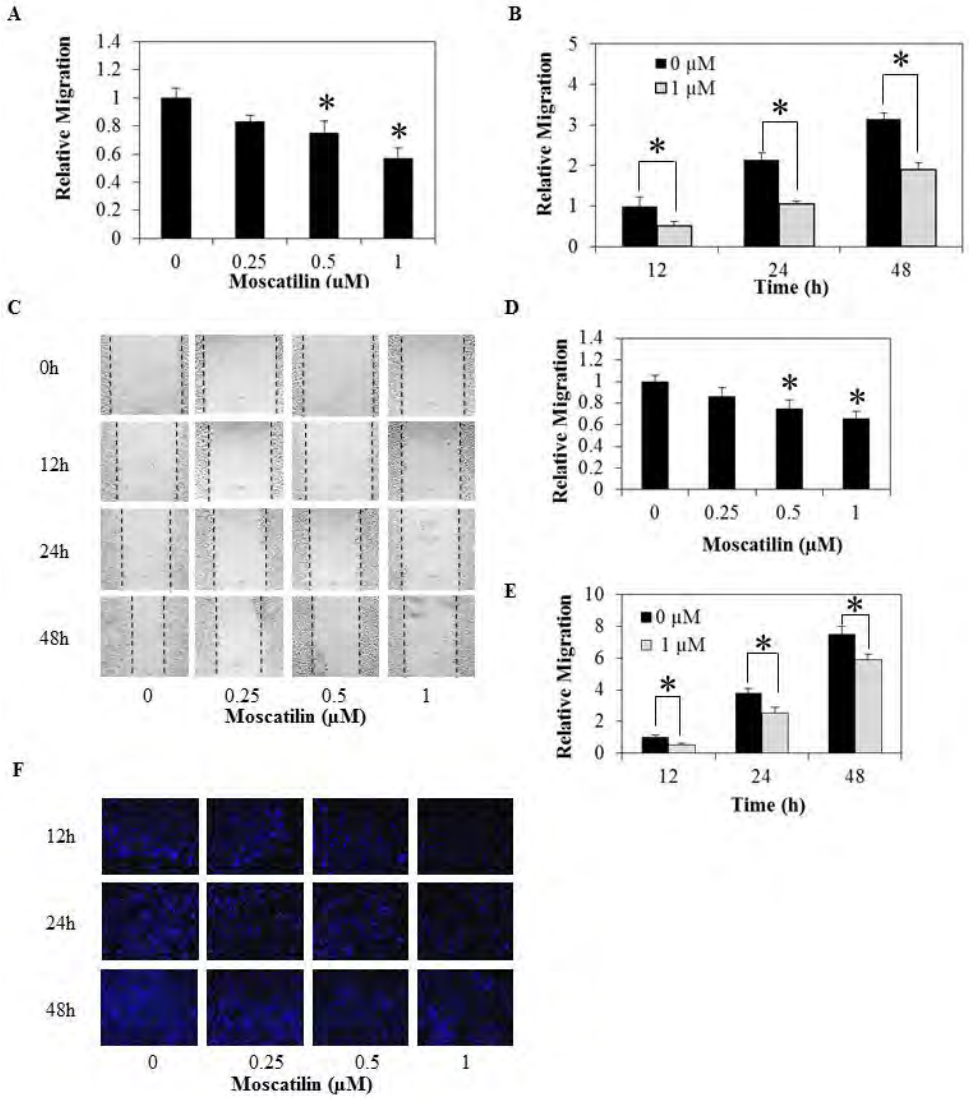


**Figure 13.** Effects of moscatilin on H23 cell migration. (A) Confluent monolayer of H23 cells were wounded using a 1-mm width tip and incubated with non-toxic dose of moscatilin (0-1 μM) for 24 h. Wound space was analyzed and represented as migration level relatively to the change of those in non-treated cells. Data represent the means ± SD (n=4). **P* < 0.05 vs. non-treated control cells. (B) Confluent monolayer of H23 cells were wounded using a 1-mm width tip and incubated with moscatilin (1 μM) or without for various times (12-48 h). Wound space was analyzed and represented as migration level relatively to the change of those in non-treated cells. **P* < 0.05 vs. non-treated control cells. (C) After indicated treatment, migrating cells in the denuded zone was photographed. (D) H23 cell migration was examined by transwell assay for 24 h. Data were plotted as an average number of cells in each field and represented the means ± SD (n=4). **P* < 0.05 vs. non-treated control cells. (E) Cells were treated with moscatilin (1 μM) or without for various times (12-48 h) on transwell. Data were plotted as an average number of cells in each field and represented the means ± SD (n=4). **P* < 0.05 vs. non-treated control cells. (F) Migratory cells at the basolateral side of membrane were stained with Hoechst33342 for 30 min and visualized under fluorescence microscopy.

*Effect of moscatilin on H23 cells invasion and filopodia formation*

To further investigate the effect of moscatilin in lung cancer cell invasion, H23 cells were treated with non-toxic concentrations of moscatilin (0-1 μM) for various times (0-48 h), and invaded cells were examined by transwell invasion assay. Figures 14A and C show that nontoxic concentrations of moscatilin retarded a number of invaded cells in a dose-dependent fashion, in which approximately 0.6- and 0.5-fold of relative invaded cells were deserved in response to 0.5 and 1 μM of moscatilin, respectively. Furthermore, moscatilin was able to impede invaded cells in the time-dependent study (Figures 14B and C).

Since filopodia has been shown to play an essential role in cell motility and invasion by protrusion at the edge of motile cells for attachment and gliding (Mattila and Lappalainen, 2008), we further clarified whether the antimigrative and antiinvasive effects of moscatilin were related to the presence of filopodia. H23 cells were treated with nontoxic concentrations of moscatilin (0-1 μM) for 24 h, and filopodia of cells was identified by phalloidin-rhodamine and sulforhodamine B staining assays. Figure 14D shows that, upon migration, motile cells exhibited filopodia protrusions accumulating at the cellular edge, in which these filopodia were dramatically decreased in response to moscatilin treatments. The above finding suggests that moscatilin inhibits filopodia formation, and subsequence impedes lung cancer cell migration and invasion.

*Moscatilin attenuates cell motility through ROS-dependent mechanism*

It has been well documented that endogenous ROS, namely, superoxide anion, hydrogen peroxide, and hydroxyl radical are continuously produced inside the living cells (Lee *et al*., 2000). Substantial studies have indicated the regulatory role of such specific ROS in cell behaviors including migration and invasion (Luanpitpong *et al*., 2010; Hung *et al*., 2012), and most evidence indicated that these specific ROS play distinguishable

roles in cell motility. In order to provide the precise mechanism of moscatilin in the regulation of cell migration, cells were treated with various concentrations of moscatilin, and cellular ROS were investigated by using $DCFH_2$-DA, specific ROS detection probe. As expected, moscatilin caused a gradual decrease of endogenous ROS level in dose- and time-dependent manners (Figure 15A). In order to identify the specific ROS involved in our tested conditions, cells were treated with moscatilin (0-1 μM) for 3 h and incubated with specific ROS detection probes: hydroxyphenyl fluorescein (HPF), amplex red and dihydroethidium (DHE). Interestingly, moscatilin shows an antioxidant effect, by which the level of $OH^{\bullet}$ is substantially decreased in response to moscatilin treatment (Figure 15B). In addition, no change was observed regarding the level of $O_2^{\bullet-}$ and $H_2O_2$ in comparison with nontreated control cells (Figures 15C and D), suggesting that endogenous $OH^{\bullet}$ is a targeted species eliminated by moscatilin. To confirm the anti-$OH^{\bullet}$ effect of moscatilin, cells were treated with specific $OH^{\bullet}$ generator (ferrous sulfate) in the presence of moscatilin for 3 h, and ROS levels were identified using $DCFH_2$-DA specific ROS detection probes. Figure 15E clearly demonstrates that an extensive increase in ROS level mediated by ferrous sulfate was in turn suppressed gradually by moscatilin in a dose-dependent fashion. This novel finding indicated that moscatilin shows a potent antioxidant against endogenous ROS, and $OH^{\bullet}$ is the most affected species.

Parallel study was conducted to investigate the relevance of antioxidant effect of moscatilin on cancer migration, and cells were preincubated with $OH^{\bullet}$ generator in the presence or absence of moscatilin treatment. Wound healing assay shows that ferrous sulfate treatment significantly enhanced the migration of cells, and the addition of moscatilin was able to abolish such an effect (Fig. 15F). These findings suggest that antimigrative effect of moscatilin was associated with its ability to suppress endogenous $OH^{\bullet}$.

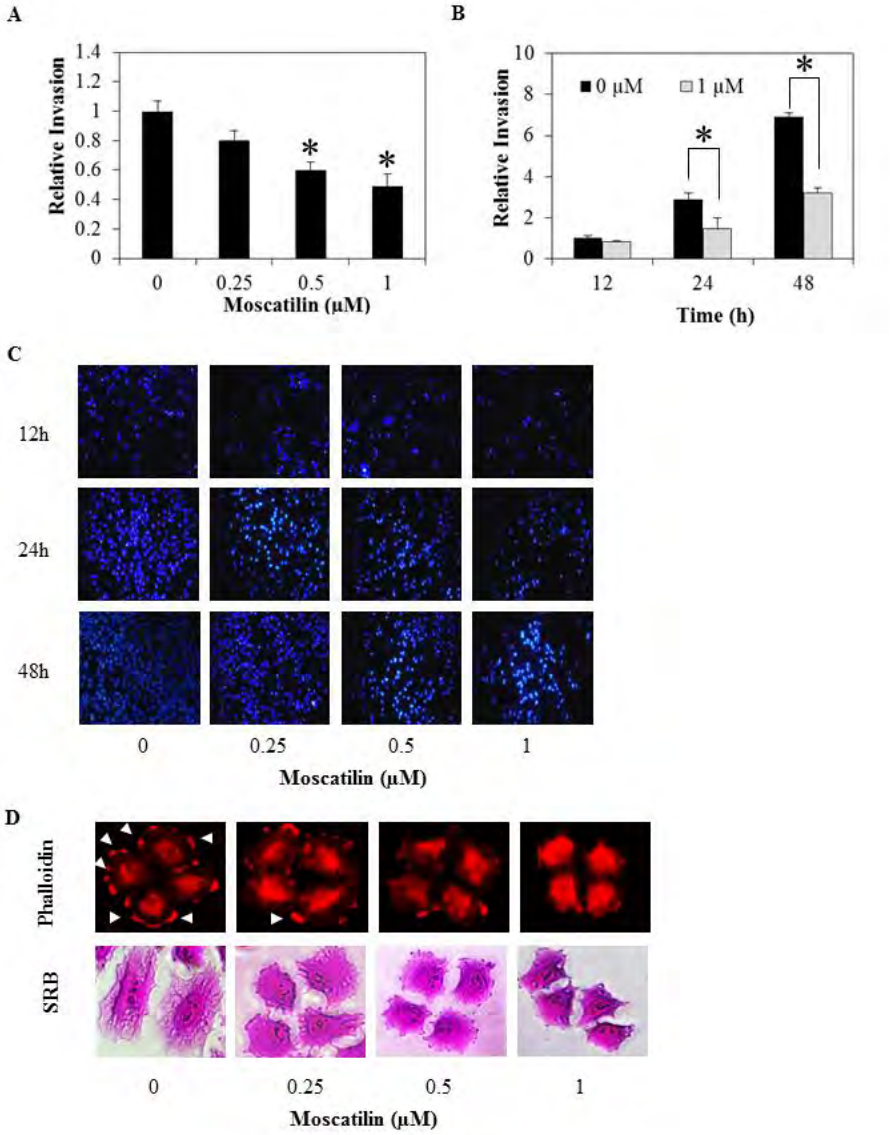


**Figure 14**. Effects of moscatilin on H23 cell invasion. (A) H23 cells were treated with various non-toxic doses of moscatilin (0-1 μM) for 24 h. (B) H23 cells were treated with moscatilin (1 μM) or left untreated as control for various times (12-48 h). Cell invasion was evaluated using transwell coated with matrigel as described under *Materials and Methods*. Invade cell across the membrane were stained with Hoechst33342 for 30 min. Data were plotted as an average number of cells in each field and represented the means ± SD (n=4). *$P < 0.05$ vs. non-treated control cells. (C) Invade cells were stained with Hoechst 33342 and visualized under fluorescence microscopy. (D) Effect of moscatilin on filopodia formation and cell morphology. After treated with non-toxic dose of moscatilin for 24 h, cells were stained with either phalloidin or sulforhodamine B and visualized under fluorescence microscope. Filopodia was indicated by arrow.

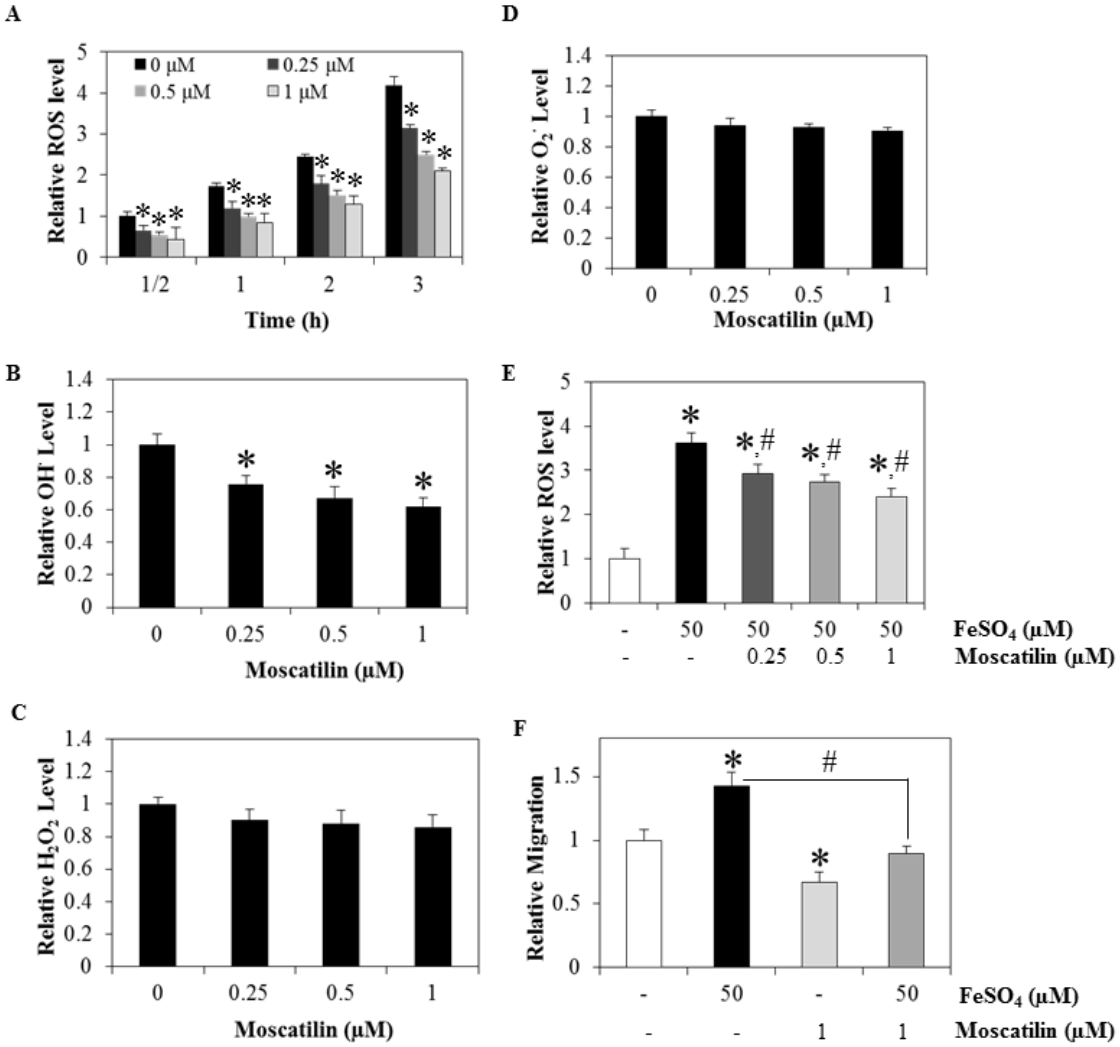


**Figure 15.** Effect of moscatilin on endogenous reactive oxygen species (ROS) generation. H23 cells were treated with various non-toxic doses of moscatilin (0-1 μM) for various times (0-3 h). (A) Endogenous cellular ROS levels were determined by dicholorofluorescein diacetate ($DCFH_2$-DA) probe. Value are mean± SD (n=4). *$P$ < 0.05 vs. non-treated control cells of each time point. (B) After indicated treatment for 3 h, cells were incubated with hydroxyphenyl fluorescein (HPF) probe. Hydroxyl radical level was detected using fluorescence microplate reader. *$P$ < 0.05 vs. non-treated control cells. (C) Hydrogen peroxide level was examined using amplex red probe. *$P$ < 0.05 vs. non-treated control cells. (D) Superoxide anion level was detected by dihydroeithidium (DHE) probe. *$P$ < 0.05 vs. non-treated control cells. (E) Cells were pre-treated with 50 μM of ferrous sulfate ($FeSO_4$) for 30 min prior to moscatilin treatments (0-1 μM) for 3 h. Endogenous ROS level were determined by using dicholorofluorescein diacetate ($DCFH_2$-DA) probe. Value are mean± SD (n=4). *$P$ < 0.05 vs. non-treated control cells. $^{\#}P$ < 0.05 vs. ferrous sulfate treated-cells. (F) Confluent monolayer of H23 cells were wounded using a 1-mm width tip and treated with moscatilin (1 μM) in the presence or absence of 50 μM of ferrous sulfate ($FeSO_4$) for 24 h. Wound space was analyzed and represented as migration level relatively to the change of those in non-treated cells. *$P$ < 0.05 vs. non-treated control cells. $^{\#}P$ < 0.05 vs. ferrous sulfate treated-cells.

*Effect of moscatilin on the FAK signaling in H23 cells*

Having shown that moscatilin suppressed the migration of the cells via hydroxyl radical attenuation, we further provided the possible underlying mechanisms involving migratory regulating proteins. Focal adhesion kinase (FAK), ATP-dependent tyrosine kinase (Akt), p44/42 mitogen-activated protein kinase (ERK1/2), and cell division cycle 42 (Cdc42) were reported to implicate cell motility in several studies (Shukla *et al*., 2007; Mattila and Lappalalainen, 2008; Teranishi, Kimura and Nishida, 2009); therefore, the expression and activated level of the proteins were investigated. Cells were treated with moscatilin for 24 h, and the expression levels of these proteins including activated FAK (phosphorylated FAK, Tyr 397), FAK, activated Akt (phosphorylated Akt, Ser 473), Akt, activated ERK1/2 (phosphorylated ERK1/2, Thr202/Tyr204), ERK1/2 and Cdc42 were determined by Western blotting. Figure 16 shows that treatment with moscatilin caused a substantially downregulation of activated FAK and activated Akt as compared to nontreated control. In addition, activated ERK1/2, ERK1/2, and Cdc42 are not affected by moscatilin. These results suggest that moscatilin attenuated the activation of migrating-related proteins FAK and Akt, in accordance with the ability of such agent on lowering endogenous ROS.

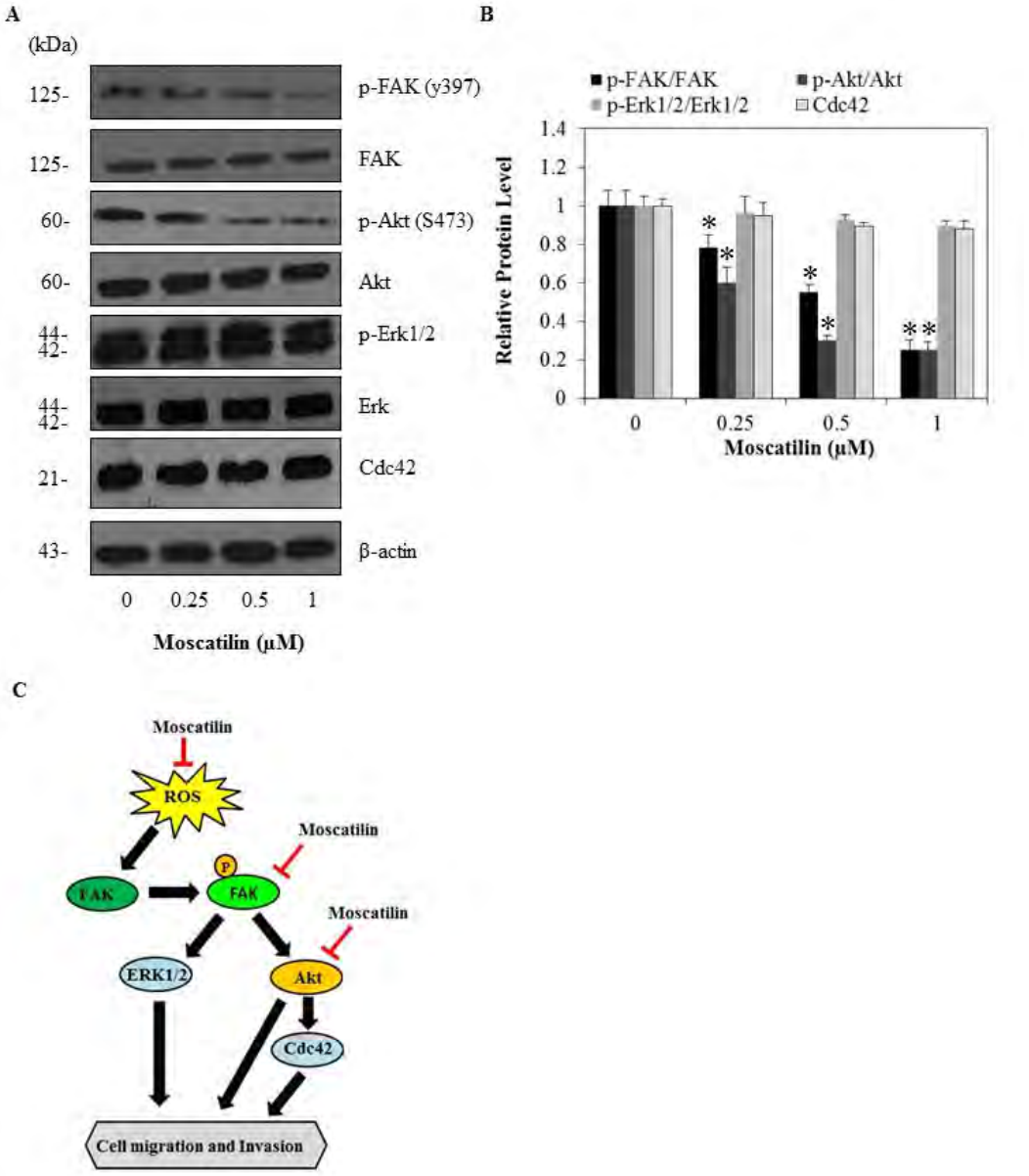


**Figure 16.** Effect of moscatilin on migratory-related proteins. (A) H23 Cells were treated with various non-toxic doses of moscatilin (0-1 μM) for 24 h and analyzed for protein expression by using western blot analysis as described under *Materials and Methods*. Cells were collected and analyzed for phosphorylated-FAK (Tyr 397), FAK proteins, phosphorylated -Akt (Ser 473), Akt, phosphorylated -Erk1/2 (Thr202/Tyr204), Erk1/2 and Cdc42 proteins. Blots were reprobed with β-actin to confirm equal loading. (B) The immunoblot signals were quantified by densitometry and mean data from four independent experiments were presented. Values are means of samples ± SD. **P* < 0.05 vs. non-treated control cells. (C) A schematic diagram summarizes the inhibitory effect of moscatilin on lung cancer cell migration and invasion. Moscatilin suppresses ROS production and consequently attenuates the activation of FAK and Akt in H23 cells.

**Discussion**

Cancer metastasis is a complex multistep process whereby cancer cell migration and invasion are crucial in determining the capability of cancer to metastasize. Cancer migration is characterized by the movement of cancer to other places which initiates by the dynamic change of cytoskeleton including protrusion of cell membrane and actin-myosin contraction. Even though the invasion of cancer cells was shown to share certain molecular mechanisms with cell migration, invasion is more focused on the ability of cancer to disrupt basement membrane and extracellular matrix by secreting the proteolytic enzyme to destruct the meshwork of basement membrane, prior to migration through surroung tissue (Fidler, 2002). Most of metastasis cancer cells exhibit these aggressive behaviors which limit the effectiveness of cancer therapy and result in high mortality rate of lung cancer patients (Ray and Jablons, 2009). Many studies have been conducted in the past decade to explore biological agents that have an ability to inhibit cancer metastasis. According to numerous researches, moscatilin, a major constituent of *Dendrobium pulchellum*, is one such interested in its anti-mutagenic activity against several cancer types (Ho and Chen, 2003; Chen *et al*., 1994). We also provided further evidence supporting the promising role of this natural compound for treatment of metastasis cancers. Our findings show that nontoxic doses of moscatilin were able to inhibit lung cancer cell migration and invasion (Figures 15 and 16). Our work also reported herein for the first time that such an inhibitory effect was involved with the potential of moscatilin to attenuate endogenous ROS which $OH^{\bullet}$ was identified to be an affected species.

The role of ROS in cancer behavior has been well described including regulation of cell motility and invasiveness (Storz, 2005; Luanpitpong *et al*., 2010). Recently, specific ROS, $O_2^{\bullet -}$ and $H_2O_2$ were shown to exhibit a negative regulatory effect on cell

migration and invasion, whereas $OH^{\bullet}$ encourages such activities (Luanpitpong *et al*., 2010). Previously, moscatilin was reported to have antioxidant effect (Zhang *et al*., 2007), and we further found that this substance reduced endogenous $OH^{\bullet}$ and thus inhibited migratory action of the cells. Consistent with previous study, we found that the addition of ferrous sulfate promoted cancer cell motility, which can be conversed by treatment with moscatilin.

Emerging evidence showed that several signaling molecules such as focal adhesion kinase (FAK), Akt/phosphatidylinositol-3-kinase (PI3K) and p44/42 Mitogen-activated protein kinases (ERK1/2) play enhancing roles on motility of cells (Mitra and Schlaepfer, 2006; Si *et al*., 2012). Recently, focal adhesion kinas (FAK) pathway has gained increasing attention as migratory-related proteins (Si *et al*., 2012). During cell motility, FAK accumulated at the site of intergrin and the phosphorylated form of FAK was shown to serve as binding site for Src (Shukla *et al*., 2007). FAK-Src complexes enhance actin polymerization and filopodia formation through Cdc42-dependent mechanism (Shukla *et al*., 2007; Mattila and Lapplainen, 2008). In addition, Akt and ERK signaling were implicated in cancer migration and invasion, of which the suppression of either their expressions or activity by silencing plasmid or specific inhibitor was able to attenuate these activities (Teranishi *et al*., 2009). Accumulative studies have demonstrated that these mentioned proteins function independently from each other (Peng *et al*., 2005), and some evidence showed the linkage of them on cell motility (Hayahi *et al*., 2008). FAK activation was shown to mediate Akt phosphorylation which resulted in cell movement. According to this report, the reduction of Akt activation might be a consequent event as downstream effector in response to moscatilin-attenuating FAK phosphorylation. Even ERK and Cdc42 were indicated to potentiate cells to migrate and invade (Mattila and Lappalainen, 2008; Si *et al*., 2012), this study demonstrated that

moscatilin impeded migratory activity of H23 cells via ERK- and Cdc42-independent mechanisms. These results provide a mechanistic insight into the mechanism of moscatilin on cancer cell migration and invasion through suppression of endogenous ROS and FAK and Akt activation.

**Conclusion**

In conclusion, we reported a novel finding on moscatilin-suppressing migratory behavior of lung cancer cells, and its molecular mechanism. The migrative-inhibitory effect of moscatilin was through an attenuation of endogenous $OH^{\bullet}$. In addition, moscatilin reduced FAK and Akt activation, which at least in part, is responsible for its antimigratory effects. Since cell motility and invasion were critical implicated in cancer metastasis, this study thus provides information and highlights potential of this natural-based compound for clinical use to overcome cancer metastasis.

***Abbreviations**:* Akt, ATP-dependent tyrosine kinase; Cdc42, cell division cycle 42; $DCFH_2$-DA, dichlorfluorescein-diacetate; DHE, dihydroethidium; ERK1/2, extracellular signal-regulated kinase; FAK, focal-adhesion kinase; HPF, hydroxyphenyl fluorescein; $H_2O_2$, hydrogen peroxide; MTT, 3-(4,5-dimethylthiazol-2-yl)-2,5-diphenyltetrazolium bromide; $OH^{\cdot}$, hydroxyl radical; $O_2^{\cdot-}$, superoxide; p-Akt, phosphorylated Akt; PBS, phosphate-buffered saline; p-ERK1/2, phosphorylated-ERK1/2; p-FAK, phosphorylated-FAK; PI**,** propidium iodide; ROS, reactive oxygen species; TBST, tris-buffered saline with 0.1% Tween

# CONCLUSION

In this study, sixteen phenolic compounds were isolated from the methanol extracts of *Dendrobium pulchellum* and *D. ellipsophyllum*. These compounds were characterized as chrysotobibenzyl, chrysotoxine, crepidatin, moscatilin, fimbriatone, (-)-shikimic acid, liriodendrin, 5,7-dihydroxy-chromen-4-one, 4,5-dihydroxy-2,3-dimethoxy-9,10-dihydrophenanthrene, 4,4′-dihydroxy-3,5-dimethoxybibenzyl, 4,5,4′-trihydroxy-3,3′-dimethoxybibenzyl, (2*S*)-homoeriodictyol, (2*S*)-eriodictyol, chrysoeriol, phloretic acid and luteolin. Moscatilin is only one compound which was found from both plant species. These isolates were evaluated for cytotoxic and anti-metastatic activities against human lung cancer cells. It was found that chrysotobibenzyl, chrysotoxine, crepidatin, moscatilin, 4,4′-dihydroxy-3,5-dimethoxybibenzyl, 4,5,4′-trihydroxy-3,3′-dimethoxybibenzyl, chrysoeriol and luteolin exhibited appreciable cytotoxic and anti-metastatic effects. Moscatilin, the strongest cytotoxic compounds from *D. pulchellum*, was selected for further evaluated for its mechanisms of action. The present study demonstrates that moscatilin was able to inhibit human lung cancer cell migration and invasion. The inhibitory effect of moscatilin was associated with an attenuation of endogenous reactive oxygen species (ROS), in which hydroxyl radical ($OH^{\bullet}$) was identified as a dominant species in the suppression of filopodia formation.

## SUGGESTION FOR FURTHER WORKS

In this study, we focus on cytotoxic effect of isolated compounds from *Dendrobium* spp. against human lung cancer cells. These compounds will be further evaluated of cytotoxic activity on other lung cancer cells. Also, the mechanisms of anti-metastatic compounds are necessary to be studied. If possible, anti-metastatic effects of moscatilin in animal model will be investigated.

## REFERENCES

Boisvert, A. K., Longmate, W., Abel, E.V. and Aplin, A. E. 2009. Mcl-1 is required for melanoma cell resistance to anoikis. Molecular Cancer Research **7**:549-556.

Brazil, D. P. and Hemmings, B. A. 2001. Ten years of protein kinase B signaling: a hard Akt to follow. Trends in Biochemical Science 26: 657-664.

Bureau of Policy and Strategy, Ministry of Public Health. Ten-first deaths 2009 [Online]. Available from: http://bps.ops.moph.go.th/index.php?mod=bps&doc=5. [Accessed November 18, 2013].

Chanvorachote, P. and Pongrakhananon, V. 2013. Ouabain downregulates Mcl-1 and sensitizes lung cancer cells to TRAIL-induced apoptosis. American Journal of Physiology-Cell Physiology 304: 263-272.

Chen, C.C., Wu, L.G., Ko, F.N. and Teng, C.M. 1994. Antiplatelet aggregation principles of *Dendrobium loddigesii*. Journal of Natural Products 57:. 1271-1274.

Chen, T.H., Pan, S.L., Liao, C.H., Guh, J.H., Wang, S.W., Sun, H.L., Liu, Y.N., Chen, C.C., Shen, C.C., Chang, Y.L. and Teng, C.M. 2008a. Moscatilin induces apoptosis in human colorectal cancer cells: a crucial role of c-Jun $NH_2$-terminal

protein kinase activation caused by tubulin depolymerization and DNA damage. Clinical Cancer Research 14: 4250-4257.

Chiarugi, P. and Giannoni, E. 2008. Anoikis: a necessary death program for anchorage-dependent cells. Biochemical Pharmacology 76:1352-1364.

Deyama, T. 1983. The constituents of Eucommia ulmoides Oliv. Isolation of (+)-medioresinol di-O-$\beta$-D-glucopyranoside. Chemical & Pharmaceutical Bulletin 31: 2993-2997.

Du, Q., Jerz, G., and Winterhalter, P. 2004. Preparation of three flavonoids from the bark of *Salix alba* by high-speed countercurrent chromatographic separation. Journal of Liquid Chromatography & Related Technologies 27: 3257-3264.

Encarnación, D. R., Nogueiras, C. L., Salinas, V. H. A., Anthoni, Nielsen, U. P. H., and Christophersen, C. 1999. Isolation of eriodictyol identical with huazhongilexone from *Solanum hindsianum*. Acta Chemica Scandinavica 53: 375-377.

Fidler, I. J. 2005. The organ microenvironment and cancer metastasis. Differentiation 70: 498-505.

Frisch, S. M. and Francis, H. 1994. Disruption of epithelial cell-matrix interactions induces apoptosis. The Journal of Cell Biology 124: 619-626.

Golstein, P., and Kroemer, G. 2007. Cell death by necrosis: towards a molecular definition. Trends in Biochemical Sciences 32: 37-43.

Guanghua, Z., Zhanhe, J., Wood, J. J. and Wood, H. P. 2009. *Dendrobium* Swartz. Flora of China 25: 367.

Halim, H., Chunhacha, P., Suwanborirux, K. and Chanvorachote, P. 2011. Anti-cancer and antimetastatic activities of renieramycin M, a marine tetrahydroisoquinoline

alkaloid, in human non-small cell lung cancer cells. Anticancer Research 31: 193-201.

Hanahan, D. and Weinberg, R. A. 2000. The hallmarks of cancer. Cell 100: 57-70.

Hayashi, H., Tsuchiya, Y., Nakayama, K., Satoh, T., Nishida, E. 2008. Down-regulation of the PI3-kinase/Akt pathway by ERK MAP kinase in growth factor signaling. Genes Cells 13: 941-947.

Ho, C.K. and Chen, C.C. 2003. Moscatilin from the orchid *Dendrobium loddigesii* is a potential anticancer agent. Cancer Investigation 21: 729-736.

Hossain, M. M. 2011. Therapeutic orchids: traditional uses and recent advance-an overview. Fitoterapia 82: 102-140.

Huang, Q., Lu, G., Shen. H. M., Chung, M. C. M. and Ong, C. N. 2007. Anti-cancer properties of anthraquinones from rhubarb. Medicinal Research Reviews 27: 609-630.

Hung, W.Y., Huang, K.H., Wu, C.W., Chi, C.W., Kao, H.L., Li, A.F.Y., Yin, P.H. and Lee, H.C. 2012. Mitochondrial dysfunction promotes cell migration via reactive oxygen species enhanced beta5-integrin expression inhuman gastric cancer SC-M1 cells. Biochimica et Biophysica Acta 1820: 1102-1110.

Hynes, R. O. 1999. Cell adhesion: old and new questions. Trends in Cell Biology 9: M33-37.

Hu, J., Fan, W., Dong, F., Miao, Z. and Zhou, J. 2012. Chemical components of *Dendrobium chrysotoxum*. Chinese Journal of Chemistry 30: 1327-1330.

Ishimaru, K., Nonaka, G. I. and Nishioka, I. 1987. Gallic acid esters of proton-quercitol, quinic acid and (-)-shikimic acid from *Quercus mongolica* and *Q. myrsinaefolia*. Phytochemistry 26: 1501-1504.

Katerere, D. R., Gray, A. I., Nash, R. J., and Waigh, R. D. 2012. Phytochemical and antimicrobial investigations of stilbenoids and flavonoids isolated from three species of Combretaceae. Fitoterapia 83: 932-940.

Kim, H. Y., Jung, S. K., Byun, S., Son, J. E., Oh, M. H., Lee, J., Kang, M. J., Heo, Y. S., Lee, K. W. and Lee, H. J. 2013. Raf and PI3K are the molecular targets for the anti-metastatic effect of luteolin. Phytotherapy Research 27: 1481-1488.

Lee, H.C., Yin, P.H., Lu, C.Y., Chi, C. and Wei, Y.H. 2000. Increase of mitochondria and mitochondrial DNA in response to oxidative stress in human cells. Biochemical Journal 348: 425-432.

Lei, Y., Huang, K., Gao, C., Lau, Q. C., Pan, H., Xie, K., Li, J., Liu, R., Zhang, T., Xie, N., Nai, H.S., Wu, H., Dong, Q., Zhao, X., Nice, E. C., Huang, C. and Wei, Y. 2011. Proteomics Identification of ITGB3 as a key regulator in reactive oxygen species induced migration and invasion of colorectal cancer cells. Molecular & Cellular Proteomics 10: 1-16.

Li, S., He, S., Zhong, S., Duan, X., Ye, H., Shi, J., Peng, A. and Chen, L. 2011. Elution-extrusion counter-current chromatography separation of five bioactive compounds from *Dendrobium chrysotosum* Lindl. Journal of Chromatography A 1218: 3124-3128.

Li, Y. M., Wang, H. Y. and Liu, G. O. 2001. Erianin induces apoptosis in human leukemia HL-60 cells. Acta Pharmacologica Sinica 22: 1018-1022.

Liu, Y. L., Ho, D. K. and Cassady, J. M.. 1992. Isolation of potential cancer chemopreventive agents from *Eriodictyon californicum*. Journal of Natural Products 55: 357-363.

Liu, Y. N., Pan, S. L., Peng, C. Y., Huang, D. Y., Guh, J. H., Chen, C. C., Shen, C. C. and Teng, C. M. 2009. Moscatilin repressed lipopolysaccaride-induced HIF-1 alpha accumulation and NF-kappaB activation in murine RAW264.7 cells. Shock 33: 70-75.

Luanpitpong, S., Talbott, S.J., Rojanasakul, Y., Nimmannit, U., Pongkrakhananon, V., Wang, L. and Chanvorachote, P. 2010. Regulation of lung cancer cell migration and invasion by reactive oxygen species and caveolin-1. Journal of Biological Chemistry 285: 38832-38840.

Majumder, P. L. and Chatterjee, S. 1989. Crepidatin, a bibenzyl derivative from the orchid *Dendrobium crepidatum*. Phytochemistry 28: 1986.1988.

Majumder, P. L. and Sen, R. C. 1987. Moscatilin, a bibenzyl derivative from the orchid *Dendrobium moscatum*. Phytochemistry 26: 2121-2124.

Mattila, P. K., Lappalainen, P. Filopodia: molecular architecture and cellular functions. Nature Reviews Molecular Cell Biology 9: 446-454.

Mitra, S. K., and Schlaepfer, D. D. 2006. Integrin-regulated FAK-Src signaling in normal and cancer cells. Current Opinion in Cell Biology 18: 516-523.

Mori, S., Chang, J. T., Andrechek, E.R., Matsumura, N., Baba, T., Yao, G., Kim, J.W., Gatza, M., Murphy, S. and Nevins, J. R. 2009. Anchorage-independent cell growth signature identifies tumors with metastatic potential. Oncogene 28*:* 2796-2805.

Muangman, S., Thippornwong, M. and Tohtong, H. 2005. Anti-metastatic effects of curcusone B, a diterpene from *Jatropha curcas*. In Vivo 19: 265-268.

Ng, T.B., Liu, J., Wong. J.H., Ye, X., Wing Sze, S.C., Tong, Y. and Zhang, K.Y. 2012. Review of research on *Dendrobium*, a prized folk medicine. Applied Microbiology and Biotechnology 93: 1795-1803.

Ono, M., Ito, Y., Masuoka, C., Koga, H. and Nohara, T. 1995. Antioxidative constituents from Dendrobii Herba (Stems of *Dendrobium* spp.). Food Science and Technology International 2: 115-120.

Owen, R. W., Haubner, R., Mier, W., Giacosa, A., Hull, W. E., Spiegelhalder, B., and Bartsch, H. 2003. Isolation, structure elucidation and antioxidant potential of the major phenolic and flavonoid compounds in brined olive drupes. Food and Chemical Toxicology 41: 703-717.

Pai, H. C., Chang, L. H., Peng, C. Y., Chang, Y. L., Chen, C. C., Shen, C. C., Teng, C. M., Pan, S. L. 2013. Moscatilin inhibits migration and metastasis of human breast cancer MDA-MB-231 cells through inhibition of Akt and Twist signaling pathway. Journal of Molecular Medicine 91: 347-356.

Park, Y., Moon, B. H., Yang, H., Lee, Y., Lee, E., and Lim, Y. 2007a. Complete assignments of NMR data of 13 hydroxymethoxyflavones. Magnetic Resonance in Chemistry 45: 1072-1075.

Park, Y., Moon, B. H., Lee, E., Lee, Y., Yoon, Y., Ahn, J. H., and Lim, Y. 2007b. $^{1}H$ and $^{13}C$-NMR data of hydroxyflavone derivatives. Magnetic Resonance in Chemistry 45: 674-679.

Peng, S. B., Peek, V., Zhai, Y., Paul, D.C., Lou, Q., Xia, X., Eessalu, T., Kohn, W. and Tang, S. 2005. Akt activation, but not extracellular signal-regulated kinase activation, is required for SDF-1alpha/CXCR4-mediated migration of epitheloid carcinoma cells. Molecular Cancer Research 3: 227-236.

Phechrmeekha, T., Sritularak, B. and Likhitwitayawuid, K. 2012. New phenolic compounds from *Dendrobium capillipes* and *D. secundum*. Journal of Asian Natural Products Research. 14: 748-754.

Ray, M. R., and Jablons, D. M. 2009. Lung cancer metastasis novel biological mechanisms and impact on clinical practice, in: V. Keshamouni, D. Arenberg, and G. .Kalemkerian, (Eds.), Hallmarks of metastasis, Springer New York, New York, NY, pp. 29-46.

Reed, J. C. 2000. Mechanism of apoptosis. The American Journal of Pathology 157: 1415-1430.

Seidenfaden G. 1985. Orchid genera in Thailand XII. *Dendrobium* Sw. Opera Botanica 83: 1-295.

Shanker, M., Willcutts, D., Roth, J.A., Ramesh, R. 2010. Drug resistance in lung cancer. Lung Cancer: Targets and Therapy 1: 23-36.

Shanmugathasan, M. and Jothy, S. 2000. Apoptosis, anoikis and their relevance to the pathobiology of colon cancer. Pathology International 50: 273-279.

Shukla, S., MacLennan, G. T., Hartman, D. J., Fu, P., Resnick, M. I., Gupta, S. 2007. Activation of PI3K-Akt signaling pathway promotes prostate cancer cell invasion. International Journal of Cancer 121: 1424-1432.

Si, H., Peng, C., Li, J., Wang, X., Zhai, L., Li, X. and Li, J. 2012. RNAi-mediated knockdown of ERK1/2 inhibits cell proliferation and invasion and increases chemosensitivity to cisplatin in human osteosarcoma U2-OS cells in vitro. International Journal of Oncology 40: 1291-1297.

Siegel, R., Naishadham, D. and Jemal, A. 2012. Cancer statistics 2012. CA: A Cancer Journal of Clinicians 62: 10-29.

Sritularak, B. and Likhitwitayawuid, K. 2009. New bisbibenzyls from *Dendrobium falconeri*. Helvetica Chimica Acta 92: 740-744.

Sritularak, B., Anuwat, M. and Likhitwitayawuid, K. 2011a. A new phrenanthrenequinone from *Dendrobium draconis*. Journal of Asian Natural Prodruct Research 13: 251-255.

Sritularak, B., Duangrak, N., and Likhitwitayawuid, K. 2011b. A new bibenzyl from *Dendrobium secundum*. Verlag der Zeitschrift für Naturforschung 66c: 205-208.

Storz, P. 2005. Reactive oxygen species in tumor progession. Frontiers in Bioscience 10: 1881-1896.

Teranishi, S., Kimura, K. and Nishida, T. 2009. Role of Formation of an ERK-FAK-paxillin complex in migration of human corneal epithelial cells during wound closure in vitro. Investigative Ophthalmology & Visual Science 50: 5646-5652.

Tsai, A. C., Pan, S. L., Liao, C. H., Guh, J. H., Wang, S. W., Sun, H. L., Liu, Y. N., Chen, C. C., Shen, C. C., Chang Y. L. and Teng, C. M. 2010. Moscatilin, a bibenzyl derivative from the India orchid *Dendrobium loddigersii*, suppresses tumor angiogenesis and growth *in vitro* and *in vivo*. Cancer Letters 292: 163-170.

Wang, F., Yamauchi, M., Muramatsu, M., Osawa, T., Tsuchida, R. and Shibuya, M. 2011. RACK1 Regulates VEGF/Flt1-mediated Cell Migration via activation of a PI3K/Akt pathway. Journal of Biological Chemistry 286: 9097-9016.

Wei, D. Z., Yang, J. Y., Liu, J. W. and Tong, W. Y. 2003. Inhibition of liver cancer cell proliferation and migration by a combination of (-)-epigallocatechin-3-gallate and ascorbic acid. Journal of Chemotherapy 15: 591-595.

Wollenweber, E.,Doerr, M., Stelzer, R. and Arriaga-Giner, F. J. 1992. Lipophilic phenolics from the leaves of *Empetrum nigrum* - chemical structures and exudate localization. Botanica Acta 105: 300-305.

Yang, H., Sung, S. H. and Kim, Y. C. 2007. Antifibrotic phenanthrenes of *Dendrobium nobile* stems. Journal of Natural Products 70: 1925-1929.

Zhang, G. N., Zhong, L. Y., Annie Blight, S. W., Guo, Y. L., Zhang, C. F., Zhang, M., Wang, Z. T. and Xu, L. S. 2005. Bi-bicyclic and bi-tricyclic compounds from *Dendrobium thyrsiflorum*. Phytochemistry 66: 1113-1120.

Zhang, L., Zhou, G.Z., Song, W., Tan, X.R., Guo, Y.Q., Zhou, B., Jing, H., Zhao, S.J. and Chen, L.K. 2012. Pterostilbene protects vascular endothelial cells against oxidized low-density lipoprotein-induced apoptosis in vitro and in vivo. Apoptosis 17: 25-36.

Zhang, X., Xu, J.K., Wang, N.L., Kurihara, H. and Yao, X.S. 2008. Antioxidant phenenthrenes and lignans from *Dendrobium nobile*. Journal of Chinese Pharmaceutical Sciences 17: 314-318.